DEUTSCHES ELEKTRONEN – SYNCHROTRON

DESY 91-110
September 1991

Nucleon Structure Function at Small x

E. M. Levin

Deutsches Elektronen-Synchrotron DESY, Hamburg

and

St. Petersbourg Nuclear Physics Institute,
Gatchina, St. Petersbourg, USSR

ISSN 0418-9833

NOTKESTRASSE 85 · D-2000 HAMBURG 52

To be sure that your preprints are promptly included in the
HIGH ENERGY PHYSICS INDEX,
send them to the following (if possible by air mail):

DESY
Bibliothek
Notkestrasse 85
D–2000 Hamburg 52
Germany

DESY 91-110
September 1991

ISSN 0418-9833

NUCLEON STRUCTURE FUNCTION at SMALL x.

E. M. Levin

DESY

Notkestrasse 85, 2000 Hamburg 52, FRG

and

St. Petersbourg Nuclear Physics Institute

Gatchina, St. Petersbourg 188350, USSR

Mini-rapporteur talk at EP-HEP 91 Conference

Geneva, Switzerland, 25 July-1 August 1991

Abstract

This is a status report on the behaviour of deeply inelastic scattering in the low x region, where a new physics to be expected. It is bound to be theoretical review, since there is no data available at truely small values of x, say $x < 10^{-3}$. New data from HERA are anticipated and I am viewing on this talk as summary of the theoretical situation in the region of small x, as is just before this new area of physics will be studied experimentally. This is an extended version of the talk which was presented at EP-HEP 91 Conference.

INTRODUCTION.

In my talk I would like to address the question: What do we know about low x behaviour of deep inelastic structure functions. Let me start with the statement that I am firmly believe that the small- x physics is the most interesting and difficult problem in QCD. Only the periphery of this problem can be touched in perturbative QCD, while its kernel is a nonperturbative one.

At $x \to 0$ we deal with a dense system of partons in the weak coupling limit in which the interactions between partons are become large due to the high density of partons in spite of the fact that the coupling constant α_s is small here. The theoretical understanding of such a system of partons which will be probed experimentally at the new generation of accelerators (HERA, LHC and SSC), is relevant not only to the low -x behaviour of deep inelastic structure functions but also to the structure of typical inelastic event produced at high energy hadron- hadron interactions or in high energy ion - ion collisions, to the understanding of nuclear shadowing as well as to the problem of baryonic number noncorservation in the electroweak theory at high energies.

The fact that HERA will explore experimentally the region of low x encourages me to summarize in this talk not only our current understanding of the problem but also present the new ideas which could and should be checked experimentally in the nearest future. I am going to discuss the main ideas how to view new physics at HERA. Unfortunately, at the moment I have to restrict myself only to pure theoretical discussion since we have no experimental information on the low x region, say for $x < 10^{-3}$. I have one more reason to concentrate on theory in my talk and this is the fact that G.Mortinelli in his rapporteur talk on the status QCD at this conference did not discuss the theoretical problems encountered in perturbative QCD in the last frontier of this very powerful approach, namely in the region of small x.

At present we understand that the whole kinematical region of deeply inelastic scattering can be divided in three separate parts as shown in Fig.1. Each of these subregions has a different underlying physics and a different level of theoretical understanding. I shall discuss the situation in each subregion separately.

1. "Standard" evolution region.

This is a region with very large value of transferred momentum q^2 and moderately small values x. Deeply inelastic processes reveal here properties typical for hard processes. Namely:

1. The total cross section for virtual photon absorption is very small, $\sigma(\gamma^* N) \ll \alpha_{e.m.} \cdot \pi R_h^2$ where πR_h^2, is a typical area of the hadron. It falls down as inverse power of q^2 at large values of q^2 ($\sigma(\gamma^* N) \propto \frac{1}{q^2}$).

2. We dispose of a transparent physical language to discuss the deeply inelastic process, namely, the parton language, specially concieved for this process.

3.In this region we can apply the leading log approximation (LLA) of perturbative QCD, which leads to a linear evolution equation for deep inelastic structure function. This equation is not the same as the Gribov-Lipatov- Altarelli-Parisi one, but it is known quite well.

In summary, I think that this region is in the best theoretical shape.

2. Transition region.

In the transition region (see Fig.1) the situation changes crucially:

1. The total cross section $\sigma(\gamma^* N)$ becomes large and, near the border with "Regge" domain, even compatible with the geometrical size of the hadron at small x . It means that $\sigma(\gamma^* N) \to \alpha_{e.m.} \cdot \pi R_h^2$. In this kinematical region it depends only smoothly on $\log q^2$, that is $\sigma(\gamma^* N) \propto F(\log q^2)$.

2. The parton language can be used to discuss the main properties of our process but the interactions between parton become important. This interaction induces substantial screening (shadowing) corrections.

3. Fortunately, in this particular kinematical region the screening corrections are under theoretical control. We may go beyond the LLA and write the correct evolution equation, which becomes nonlinear. Of course, the solution of this equation is quite different from that of the GLAP equation, but the properties of this solution are quite well known.

In the course of this presentation I shall try to convince you that we have reached a good theoretical understanding of this region, especially during the two last years.

3. "Regge" domain.

The most interesting, of all, is the "Regge" domain (see Fig.1 where new physics is

anticipated.

1. The total cross section becomes huge, namely, $\sigma \propto \alpha_s \cdot \pi R_h^2 \cdot \frac{1}{\alpha_s}$.

2. Since the coupling constant of QCD remains small ($\alpha_s << 1$), we hope to be able to probe this region theoretically.

3. Unfortunately, because the parton density is so large in this region that the standard methods of perturbative QCD cannot be used.

Unfortunately, there is no real progress in the description of this region and situation could be characterized as follows: there is plenty of ideas but no results. However some experience in dealing with this domain was accumulated and this allows us to suggest some phenomenological hypothesies which could be checked experimentally. Thus, it will need a common effort of theorists and experimentalists together to clarify the understanding lying ahead physics in this domain.

I would like to address once more that the "Regge" domain is the most important from the theoretical point of view since, although the parton system is dense the coupling is weak and it gives us a chance to solve the problem. The region is also very important for practical reason, since we cannot possibly start to attack the problem of the structure of typical inelastic event in hadron-hadron interactions at high energy without understanding the deeply inelastic process in the relevant region.

To summarize, the outline of my talk look as follows. First I am going to discuss separately the situation partaining to each kinematical subregions, emphasizing the progress achieved during the last two years. Then I will consider some phenomenological aspects related mainly to estimates of the size of screening corrections. It will lead me to some aspects of the HERA physics and some problems which will be important there.

"STANDARD" EVOLUTION REGION.

Two years ago we able to calculate the basic branching process (See Fig.2) only for three separate parts of the whole phase space available for the emitted partons: for strong ordering in transverse momenta of emitted parton, or for strong ordering in their fractions of energy (x_i) or strong ordering in both .

LL(q^2)A.

The simplest case corresponds to the region of leading log approximation in $\log q^2$ (so called LL(q^2)A). In LL(q^2)A in each Feynman diagram the smallness of QCD coupling constant is compensated by large $\log q^2$. This allows to present the structure function as a series of the following type:

$$F_2(x,q^2) = \Sigma_n(\alpha_s \log q^2)^n F_n(x). \tag{1}$$

A $\ln q^2$ contribution for each integration over q_{it} in our parton cascade (see Fig,2) implies a strong ordering in transverse momenta of emitted partons. Indeed, the probability of emission of i-th parton can be written in a very simple form (at least at $x \to 0$)

$$P_i = \frac{N_c \alpha_s}{\pi} \cdot \frac{dx_i}{x_i} \cdot \frac{dq_{it}^2}{q_{it}^2} \tag{2}$$

This expression will lead to $\log q^2$ only if

$$q^2 \gg q_{nt}^2 \gg .... \gg q_{it}^2 \gg q_{(i-1)t}^2 \gg ..... \gg \frac{1}{R_p^2} = Q_0^2 \tag{3}$$

However the integration was over all possible values of x_i with constrains from energy conservation in the parton cascade. This implies that

$$x_B \leq x_n \leq ... \leq x_i \leq x_{(i-1)} \leq ..... \leq x_0 \tag{4}$$

In order for LL(q^2)A approach to be valid the following parameters to be fulfilled

$$\alpha_s \log q^2 \approx 1,\ \alpha_s \log \frac{1}{x} \ll 1,\ \alpha_s \ll 1. \tag{5}$$

It is especially important to realize the direct correlation between the kind of approximation that is used to get the evolution equation for the structure function and the kinematics of emitted partons. The LL(q^2)A leads to the standard Gribov-Lipatov-Altarelli-Parisi [1] evolution equation which allows to calculate the x-dependence of structure function at large values of q^2 if it is known at a smaller one, say at $q^2 = Q_0^2$ (see Fig.2).

LL(x)A.

In order to extract from each Feynman diagram the contribution of the order of $(\alpha_s \log \frac{1}{x})^n$ another approach was developed. In this case the structure function is as

$$F_2(x,q^2) = \Sigma_n(\alpha_s \log \frac{1}{x})^n F_n(q^2). \tag{6}$$

It is easy to see from the expression for P_i such a contribution comes only from the region with strong ordering in x, for the emitted parton but this time there is no constrains on the ordering of q_{it} values . Thus the only requirement is that

$$x_B \ll x_n \ll ..... \ll x_i \ll x_{(i-1)} \ll ..... \ll x_0 \tag{7}$$

but

$$q_{it}^2 \leq or \geq q_{(i-1)t}^2. \tag{8}$$

LL(x)A we could apply in kinematical region when

$$\alpha_s \log \frac{1}{x} \approx 1, \alpha_s \log q^2 \ll 1, \alpha_s \ll 1. \tag{9}$$

This approach leads to the Fadin -Kuraev-Lipatov equation [2], which allows to calculate the structure function at very low x, but only when the virtuality of the probe (q^2) is of the order of the initial virtuality in the parton cascade Q_0^2 (see Fig.2). In order to solve the FKL -equation, one requires the initial condition to be known as a function of q^2 at a fixed $x_B = x_0$.

LL(q^2)A + LL(x)A.

We can easily generalize both these approaches to the region where there is strong ordering for the emitted partons both in q_{it}^2 and x_i [3]. The generalization looks trivial at first sight. Indeed in the kinematical region where

$$q^2 \gg q_{tn}^2 \gg .... \gg q_{t_i}^2 \gg q_{t(i-1)}^2 \gg ..... \gg Q_0^2 \tag{10}$$

$$x_B \ll x_n \ll ..... \ll x_i \ll x_{(i-1)} \ll ..... \ll x_0 \tag{11}$$

the structure function becomes

$$F_2 = \Sigma_n \Pi_1^n P_i = \Sigma_n (\frac{N_c \alpha_s}{\pi})^n \cdot$$

$$\int_{x_B}^{x_0} \frac{dx_n}{x_n} ..... \int_{x_i}^{x_0} \frac{dx_{(i-1)}}{x_{(i-1)}} ..... \int_{x_2}^{x_0} \frac{dx_1}{x_1} \cdot \int_{Q_0^2}^{q^2} \frac{dq_{tn}^2}{q_{tn}^2} ..... \int_{Q_0^2}^{q_{t_i}^2} \frac{dq_{(i-1)t}^2}{q_{(i-1)}^2} ..... \int_{Q_0^2}^{q_{2t}^2} \frac{dq_1^2}{q_1^2} =$$

$$= \Sigma_n \frac{1}{(n!)^2} \cdot (\frac{N_c \alpha_s}{\pi} \log q^2 \log \frac{1}{x})^n \propto \exp \sqrt{4 \frac{N_c \alpha_s}{\pi} \cdot \log q^2 \log \frac{1}{x}}. \qquad (12)$$

However the main problem is to estimate the accuracy for this double logarithmic approximation (DLA). To do this let us multiply the expression for P_i by the following factor

$$1 \; + \; K_1(x, q_{it}^2) \; + \; K_2(x, q_{it}^2) \; + \; K_3(x, q_{it}^2) \qquad (13)$$

where $K_1 \to 0$ at $x \to 0$ and $K_2 \to 0$ at $q^2 \to 0$,while $K_3 \to 0$ when both x and q^2 are small($x \to 0, q^2 \to 0$. The expression for F_2 becomes now

$$F_2 \; = \; F_2(\mathrm{DLA}) \cdot$$

$$\cdot \{ 1 \; + \; \bar{n} (\frac{\int_{x_B}^1 (\frac{K_1(x,0)}{x}) dx}{\log \frac{1}{x}} \; + \; \frac{\int^{q^2} (\frac{K_2(0,q^2)}{q^2} dq^2)}{\log q^2} \; + \; \frac{\int^{q^2} \frac{dq^2}{q^2} \int_{x_B}^1 \frac{dx}{x} K_3(x, q^2)}{\log q^2 \cdot \log x} \}. \qquad (14)$$

where $\bar{n}$ is the mean multiplicity for parton cascade in DLA which is equal to $\bar{n} = \sqrt{4 \frac{N_c \alpha_s}{\pi} \cdot \log q^2 \log \frac{1}{x}}$ as calculated from the explicit form of F_2 in DLA. The interpretation of eq.(14) can be clarified from Fig.3. The subsequent corrections, induced by the K_1, K_2, K_3 terms are in fact corrections to the kernel of the branching process (or the typical ladder diagram that describes this branching process) of the order of $\alpha_s \log q^2$,$\alpha_s \log \frac{1}{x}$ or α_s,respectively. The corrections to $\frac{\Delta F_2}{F_2(\mathrm{DLA})}$ will be small only if:

1.$\bar{n} \ll \log \frac{1}{x}$ or $\alpha_s^2 \log \frac{1}{x} \ll \log q^2$ for corrections of the order of $\alpha_s \log \frac{1}{x}$.

2. $\bar{n} \ll \log q^2$ or $\alpha_s^2 \log q^2 \ll \log \frac{1}{x}$ for corrections of the order of $\alpha_s \log q^2$.

3. $\bar{n} \ll \log q^2 \log \frac{1}{x}$ or $\alpha_s^3 \ll \log q^2 \log \frac{1}{x}$ for corrections of the order α_s.

We see immediately that the most important correction is the one of the order of $\alpha_s \log \frac{1}{x}$ since it is essential for $\log \frac{1}{x} > \log^2 q^2$, while the other two remains small on the line $\log \frac{1}{x} \propto \log^2 q^2$. All these correction were taken into account in ref.[3] and such a procedure lead to the so called LL(q^2)A + LL(x)A approach. In this approach the following accuracy for F_2 is achieved:

$$F_2 \; = \; F_2(\mathrm{LL}(q^2)\mathrm{A} + \mathrm{LL}(x)\mathrm{A}) \{ 1 \; + \; O(\frac{\bar{n}}{\log q^2}) \; + \; O(\frac{\bar{n}}{\log q^2 \cdot \log \frac{1}{x}}) \} \; =$$

$$= \; F_2(\mathrm{LL}(q^2)\mathrm{A} + \mathrm{LL}(x)\mathrm{A}) \{ 1 \; + \; O(\sqrt{\alpha_s \frac{\log \frac{1}{x}}{\log q^2}}) \; + \; O(\sqrt{\alpha_s}) \}. \qquad (15)$$

Two years ago, we were able to propose the evolution equation in the kinematical region where

$$\alpha_s \log \frac{1}{x} \log q^2 \; \gg 1 \; , \alpha_s \log \frac{1}{x} \; > \; 1 \; , \; \alpha_s \log q^2 \; > \; 1 \; , \; \alpha_s \; < \; 1. \qquad (16)$$

to the right of the line $\log \frac{1}{x} \propto \log^2 q^2$.

As for today the situation in this kinematical region looks much better than was two years ago. Italian group and Webber[4,5] were able to derive and to solve the correct evolution equation in the whole "standard" evolution region. They managed to rewrite the expression for the emission of the i-th parton (P_i) in the branching process in such a way that it depends only on the kinematical variables of parton emitted in the previous stage of the parton cascade. Namely

$$dP_i \; = \; \frac{d^2 q_i}{\pi q_i^2} \Theta(q_{it} - z_{i-1} q_{(i-1)t}) \Theta(q_{it} - Q_0) dz_i \frac{N_c \alpha_s}{\pi} \Delta_{\mathrm{sud}}^{(i)} \{ \frac{1}{1 - z_i} \; + \; \frac{1}{z_i} \Delta_{\mathrm{ns}}^{(i)} \} \qquad (17)$$

where

$$\Delta_{\mathrm{sud}}^{(i)} \; = \; \exp(- \int_{(z_{i-1} q_{i-1})^2}^{q_i^2} \frac{dq^2}{q^2} \int_0^{1 - \frac{Q_0}{q}} dz \frac{N_c \alpha_s}{\pi (1 - z)}) \qquad (18)$$

$$\Delta_{\mathrm{ns}}^{(i)} \; = \; \exp(- \frac{N_c \alpha_s}{\pi} \int_{z_i}^1 \frac{dz}{z} \int_{(z q_{it})^2}^{Q_{it}^2} \frac{dk^2}{k^2} \qquad (19)$$

And the notation is explained in Fig.2.

Such a form of P_i is very well suited for Monte-Carlo simulation and allows to get a numerical solution for the evolution of parton cascades. From this branching distribution we obtain an evolution equation for the unintegrated gluon structure function

$$xG(x, q^2) \; = \; \int d^2 Q_t \phi(x, Q, Q_t), \qquad (20)$$

which looks as follows

$$\frac{\partial \phi(x, Q, Q_t)}{\partial \log Q^2} \; =$$

$$= \; \int_x^1 dz (P(z_i) - \frac{N_c \alpha_s}{\pi z_i}) \cdot \frac{1}{z} \cdot \varphi(\frac{x}{z}, \frac{Q}{z}, Q_t - \frac{1 - z}{z} Q) \; +$$

$$+ \; \int_x^1 dz (\frac{N_c \alpha_s}{\pi z} \Delta_{\mathrm{ns}}(z, \frac{Q}{z}, Q_t)) \cdot \frac{1}{z} \cdot \phi(\frac{x}{z}, \frac{Q}{z}, Q_t - \frac{1 - z}{z} Q) \qquad (21)$$

where $P(z_i)$ is the usual GLAP kernel.

It is very difficult to solve this evolution equation analytically. It is quite not a Volterra type of equation and in some sense not even evolution equation since it depends on two scales. However this equation turns into the GLAP equation for structure function for x of the order of 1 and into the FKL equation (and the GLR generalization) for the function ϕ in the region of small x. What is most important is that this correct

equation provides a smooth matching of all equations that have been discussed and describes the evolution of the parton cascade in the whole "standard" evolution region in a unique way.

It is worthwhile to mention that this correct equation provides energy conservation for deeply inelastic processes, which otherwise is violated by order of α_s both in the LL(x)A and in the LL(x)A + LL(q^2)A. This is so because the correct equation describes the region of $x \approx 1$ as well as the low-x region.

I would also like to draw attention to the fact that **two scales** of the hardness of the deep inelastic process has appeared in correct equation Q and Q_t, where Q_t is the transverse momentum of the parton which interacts with the virtual probe in the deeply inelastic scattering. The value of Q_t increases very rapidly as $x \to 0$. Indeed, the average $logQ_t^2$ is equal to

$$\langle \log Q_t^2 \rangle = \frac{\int^{Q_t^2} \log k^2 d\log k^2 \phi(x,Q,k)}{\int^{Q_t^2} \phi(x,Q,k) dlogk^2}. \tag{22}$$

The average $\langle logQ_t^2 \rangle$can de estimated in the FKL equation and it turns out that

$$\langle logQ_t^2 \rangle \propto (\alpha_s \log \frac{1}{x})^{\frac{1}{2}}. \tag{23}$$

This implies that at small x when $(\alpha_s log\frac{1}{x})^{\frac{1}{2}} \geq \log Q^2$ the hardness of the process is determined by Q_t^2 rather than Q^2. If so , in small x region we should use renormalization group approach in respect to Q_t^2.

In spite of the fact that the correct equation has not been solved analytically the result of Monte Carlo calculation [5] can provide some imformation about the solution. Here is what can be learned from the Monte Carlo calculation.

1. The solution of the correct equation coincides with the GLAP one within 5 % accuracy in the available kinematical region for both $F_2(x,q^2)$ and $xG(x,q^2)$ (see Fig.4). At first sight this fact looks very surprising and strange, since from the purely theoretical point of view, the branching process for small x is very different from the conventional ones. To understand why the two different parton cascades give the same value of the structure function the evolution path or trajectory method was developed. In terms of the branching process, the evolution path can be defined as a succession of values (x_i, Q_{ti}) (see Fig.2 for notation) for radiators on each stage of the evolution. The

structure function for a given values of x and a total emitted transverse momentum Q_t is obtained by summing over the paths that end in the neighbourhood of (x, Q_t).

The mean path and the dispersion around it has been computed analytically and also numerically, using the Monte Carlo programs of ref.[5] (see ref.[6] for details). Figure 5, which is taken from ref.[6], shows two examples of the mean paths for different initial conditions. One can see that the difference between the mean path for the GLAP evolution equation and the correct one is very small and a large fluctuation around the mean path washes out even this difference for the available x and q^2. This small difference,which is really intrinsic property of the evolution equation and does not depend, for instance, on the choice of the initial condition (see ref.[6]).

2. The correct evolution equation leads to a different structure of a typical inelastic event in deeply inelastic scattering in comparison with the GLAP equation. The multiplicity of emitted partons is larger (by 40 %) especially at the first stage of the evolution (see refs[5,6,7]).

3. In the subasymptotic kinematical region (this is actually for all experimentally accessible values of x) all predictions depend on the value Q_0. Q_0 is the initial transverse momentum from which the evolution is started (see Fig.2). For example, this effect is responsible for the result mentioned earlier that the value of the structure function turns out to be smaller than the one obtained the GLAP equation (see Fig.4). This is bad news indeed, since it means that miraculous confinement force has a direct influence on the fine structure of the behaviour of $F_2(x,q^2)$ in the region of small x. We could actually expect such an effect, because during the evolution the mean $\ln q$ increases. This means that Q_t may be either large or small, so that on each stage of evolution we touch small transverse momentum region . Deep inelastic structure function is an infrared stable value, this is the reason why Q_0 affects only its fine structure, but for the emission process the value of Q_0 plays an important role [6].

The remark is in place. All the above results were obtained from the usual way of solving of the evolution equation, where one starts at a sufficiently small $q^2 = q_0^2$ with some phenomenological function $F_{in}(x)$ as the initial condition for the evolution equation, to obtain the deep inelastic structure function for large q^2. Note that the value of q_0^2 is not the same as the value of Q_0^2. In the usual approach the evolution equation is solved in $\log q^2$ direction. However the correct evolution equation is much

richer. It allows to evolve the structure function in $\log x$ direction, as well , starting this time with $F_{in}(q^2)$ as the initial condition at fixed $x=x_0$. This latter approach may provide the information about the initial condition for the standard $\log q^2$ evolution. Of course, in this case as well some model is needed for hadron to specify $F_{in}(q^2)$ for all values of q^2. One could think of starting from the constituent quark model as was suggested by Gluck, Reya and Vogt [8]. Personally, I am convinced that he evolution in $\log x$ is correct realization of this nice idea.

Let us discuss the evolution in $\ln x$ direction in more details, since it gives us a new information about possible initial condition for the usual (GLAP) evolution. In the region of very small x the correct evolution equation coinsides with the FKL equation but with running coupling constant (α_s). We can even suggest the analitical expression for the Green function ($G_y(y-y_0, r-r_0)$) or for the solution with the initial condition: at $y=y_0$ $G_y=\delta(r-r_0)$ [37].(Here $y=\ln(1/x_B)$ and $r=\ln(q^2/\Lambda^2)$, y_0 and r_0 correspond to the initial values of x_0 and Q_0^2 in our parton cascade (see Fig.2).) This expression looks very complicated, but we can answer some questions using it. For example, we can conclude that the usual diffusion solution takes the form:

$$G_y(y-y_0, r-r_0) = \frac{\sqrt{Q_0^2}}{\sqrt{q^2}} \cdot \frac{1}{\sqrt{\pi\Delta\omega_0(y-y_0)}} \cdot$$

$$\cdot exp\{\frac{2\omega_0 r_0(y-y_0)}{r+r_0} - \frac{(r-r_0)^2(r+r_0)}{8\Delta\omega_0 r_0(y-y_0)}\}.$$

However this solution can be derived from the exact expression only if:

$$(y-y_0) \ll \frac{1}{\omega_0\Delta^{\frac{1}{3}}} \cdot (\frac{r+r_0}{2})^{\frac{5}{3}},$$

and

$$(y-y_0) \gg \frac{2}{\omega_0(r+r_0)},$$

where

$$\omega_0 = \frac{\alpha_s(Q_0^2)N_c}{\pi} \cdot 4\ln 2, \quad \Delta = \frac{14\xi(3)}{4\ln 2}.$$

It means that we can use the above simple formula for the deep inelastic structure function only in the very limited range of x. In particular, for the standard case $Q_0^2 = 5GeV^2$ and $\Lambda = 100MeV$ for $r \to r_0$ this range is

$$2 \leq y - y_0 \leq 3.$$

This conclusion is very important especially for "hot spot" hunting at HERA which I am going to discuss later.

To conclude,I am glad to say that this region now is in the best theoretical shape. The correct evolution equation is the most important theoretical achievement during the last two years, not only what conserns the deep inelastic domain but in the perturbative QCD as a whole.

Next steps.

Let me now formulate what is still needed for a better understanding of the "standard" evolution region.

1. We should try to accumulate more experience in the solution of the correct equation in the $\log x$ direction using different models for hadron as an input.

2. We are well prepared for the calculation of the next order corrections to the correct evolution equation. Till now only corrections to the GLAP equation have been discussed [9]. These corrections take into account the interactions between the emitted partons and such calculations are need to determine the boundary line between "standard" evolution region and transition region (see Fig.1). I must admit that it is really a very difficult task!

TRANSITION REGION.

Unitarity.

Before I shall describe the situation in the transition region, let me discuss a more or less formal argument arising from the unitarity constraint, which show that physics at low-x region should be quite different from what it is in the "standart" evolution region.

Indeed, unitarity tells us that the total cross section for virtual photon absorption should be smaller than the size of a hadron.

$$\sigma(\gamma^* N) \ll \pi R_h^2 \tag{24}$$

We can express $\sigma(\gamma^* N)$ through the deep inelastic structure function $xD(x,q^2$ ($F_2 =$

$xD(x.q^2)$) :

$$\sigma(\gamma^* N) = \frac{\alpha_{em}}{q^2} \cdot xD(x,q^2) \tag{25}$$

However, we have shown previously that the value of the structure function is expected to increase very rapidly when $x \to 0$. Using the DLA result (see eq. (12)), we can rewrite the unitarity constraint in the following way:

$$\frac{\alpha_s(q^2)}{q^2} \cdot \exp\sqrt{4\frac{N_c\alpha_s}{\pi} \cdot \log q^2 \log\frac{1}{x}} \ll \pi R_N^2. \tag{26}$$

Here we put α_{em} has been replaced by α_s since the probe can be also a virtual gluon not only a photon.

From this expression alone one can conclude that **unitarity will be violated** [3] for

$$x < x_{cr} \tag{27}$$

$$\log\frac{1}{x_{cr}} = \frac{b}{16N_c} \cdot \log^2 q^2 \tag{28}$$

We used the fact that $\alpha_s = \frac{4\pi}{b\log(q^2/\lambda^2)}$, and $b = \frac{11}{3}N_c - \frac{2}{3}n_F$ Therefore unitarity violates even for large (or even for very large) values of q^2 when $x < x_{cr}$ and clearly the miraculous confinement force can not prevent this phenomena. Thus that we have to look for the origin of such a violation inside perturbative QCD.

Structure of the parton cascade.

To understand what phenomena were missed in the LLA, let us consider the structure of the parton cascade for a fast hadron moving along the z- axis of our coordinate system. In deeply inelastic scattering the photon is the probe that measures the parton distribution of the hadron, but the partons exist in the free hadron, independently of any scattering process. Of course, the parton distribution describes only that part of the wave function of the hadron which becomes dominant in a hard process.

Even a slight glance at the picture in Fig.6. shows that the number of partons becomes extremely large at $x \to 0$, since each parton can decay in many daughter partons. Let us look at the distribution of partons in the transverse plane.

Our probe (photon) feels those partons whose size is of the order of $\frac{1}{q^2}$.

1. At $x \sim 1$ we have only several partons that are distributed in the hadronic disc. Let's take q^2 such that

$$r_p^2 \approx \frac{1}{q^2} \ll R_h^2. \tag{29}$$

The distance between partons in the transverse plane is much larger than their size. We can neglect the interaction between partons. The only process which is essential here is the emission of partons that is taken into account in the usual evolution equation.

2. For smaller x the number of partons increases and at some value of $x = x_{cr}$ partons start to populate densely the whole disc of the hadron.

3. For $x < x_{cr}$ partons must overlap spatially and begin to interact in a whole disc that they occupy. For such small x- values the processes of recombination and annihilation of parton should be as essential as well as their emission. However these processes were completely omitted in LLA.

Let us introduce a parameter (W) which tells us at what value of x the interaction between parton enter in the game [3], defined as follows

$$W = 4\pi\frac{\alpha_s}{q^2} \cdot \frac{xG(x,q^2)}{\pi R_h^2}, \tag{30}$$

where d xGx, q^2 is the number of partons (gluons) n_G per unit of rapidity $y = \log\frac{1}{x}$.

$$xG(x,q^2) = \frac{dn_G}{dy} \tag{31}$$

The first factor is the total cross section of parton annihilation in the parton cascade. The second factor is the density of partons in the transverse plane.

The parameter W is the probability of parton recombination in the parton cascade. Unitarity implies that this probability should be smaller than 1. Therefore, the interaction between partons must become important when

$$W \approx 1. \tag{32}$$

That is when the number of gluons becomes

$$xG(x,q^2) \approx \frac{1}{4\alpha_s} R_h^2 q^2 \tag{33}$$

For so small x, when $W \approx 1$ the structure of the parton cascade should be the result of competition of two main processes: the emission of gluons that is proportional to the density of partons (ϕ) with fixed transverse momentum and the annihilation of gluons with probability proportional to ϕ^2 (see Fig.7).

$$\phi = 4\pi \cdot \frac{dxG(x,q^2)}{dq^2} \cdot \frac{1}{\pi R_h^2} \approx \frac{4\pi xG(x,q^2)}{q^2\pi R_h^2}. \tag{34}$$

The simple parton picture allows to write the equation that takes properly into account these processes. Indeed, the number of partons in a cell of the phase space $(\Delta y.\Delta \log q^2)$ increases due to emission and decreases as result of annihilation. As an outcome the balance of particles for this cell looks as follows:

$$\frac{\partial^2 \phi}{\partial y \partial \log q^2} = \alpha_s \phi - \text{Const} \cdot \alpha_s^2 \phi^2. \tag{35}$$

Here the total cross section for gluon - gluon annihilation was written as $\sigma(GG \to G) =$ Const α_s^2.

We can rewrite this equation in terms of $xG(x,q^2)$:

$$\frac{\partial^2 xG(x,q^2)}{\partial \log \frac{1}{x} \partial \log q^2} = \alpha_s xG(x,q^2) - \alpha_s^2 \cdot \frac{\text{Const}}{q^2 R_h^2} \cdot (xG(x,q^2))^2. \tag{36}$$

The equation is exactly the same as one we has suggested many years ago [3] from analysis of Feynman diagrams in the DLA limit. As it happens, even today the same kind of analysis to calculate the value of Const and to determine the kinematical region where such simple equation holds.

Feynman diagrams.

Let me describe the main ideas behind analysis of the Feynman diagrams which contribute to deeply inelastic processes at $x \to 0$. The next order corrections to the parton density ϕ in LLA can be estimated to be proportional to (see eq.(14).)

$$\frac{\Delta \phi}{\phi_{\text{LLA}}} \propto \alpha_s \cdot \bar{n}_G, \tag{37}$$

where n_G is the mean parton (gluon) multiplicity. In the LLA as was discussed previously n_G becomes large at $x \to 0$, thus we expect a large correction. On the other hand, when the next order correction is calculated in the framework of Feyman diagrams, the correction comes out to be proportional not to the overall parton multiplicity but to the population of cells in the ladder containing the interacting parton. This is so, because in the LLA the probe interacts with only one parton, the only one particular chain in the branching process, the one containing the interacting parton is affected (Fig.8) and all the others gather back and contribute to the renormalization of the ladder rung masses. The existing of the large number of the chains in the parton cascade is reflected in the large value of the deep inelastic structure function since the probe can interact with a parton from any of the subbranching processes. All these properties are

inherent to the LLA ladder Feyman diagram. The next order correction to this LLA ladder diagram is proportional to the number of possible interactions between partons in the "interacting" chain or to the number of cells in the ladder diagram.

We have to look for other type of contributions that are large and proportional to $dn_G/d\log\frac{1}{x} = xG(x,q^2)$. Another choice is to take into account those diagrams in which the probe interacts with at least two partons. We would like to indentify those diagrams which in the next order a contribution such that

$$\frac{\Delta \phi}{\phi_{\text{LLA}}} \propto \alpha_s \cdot \frac{\phi_{\text{LLA}}}{\pi R_h^2} \approx W. \tag{38}$$

Since ϕ increases very rapidly at $x \to 0$ such a correction must be calculate in the first place and only then the other next order corrections can be estimated. The following parameters are used to classify the Feynman diagrams:

$$\alpha_s \ll 1, \ \alpha_s \log \frac{1}{x} > 1, \alpha_s \log q^2 > 1, \tag{39}$$

but

$$\alpha_s n_{(\text{ladder cells})} < 1, \ W \leq 1. \tag{40}$$

A new technique was developed in ref.[3] to calculate the corrections of the order W^n. In this technique we reduce the problem to the calculation of the LLA ("ladder") diagrams and their interactions by introducing only new vertices for those "ladder" interactions which we are able to calculate in perturbative QCD. This long sentence contains at least two non trivial statements. First we claim that we can introduce vertices which are local in rapidity and transverse momemtum, second our integration over transverse momenta is concentrated in a region of sufficiently large values of transverse momentum such that we are able to use perturbative QCD to calculate the vertices.

The result of such an analysis leads us to so called "fan" diagrams (see Fig.9) which are responsible for deeply inelastic scattering in the transition region. These diagrams can be also generated by using a nonlinear equation, the simplest version of which has been discussed in the previous section.

Nonlinear evolution equation.

Let me introduce the nonlinear (GLR) equation in the form in which the LLA branching process is calculated in the GLAP equation (see ref.[3] for more details and

a more sophisticated version of the GLR equation).

$$g(x,q^2) = \int^{q^2} \frac{dq'^2}{q'^2} \int_0^1 dz \, \frac{\alpha_s(q'^2)}{4\pi} \cdot P_G^G(z) \cdot g(\frac{x}{z}, q'^2) - \\ - \frac{9}{32} \cdot \int^{q^2} \frac{dk^2}{k^4} \int^{\log\frac{1}{x} d\log\frac{1}{x'}} \alpha_s^2(k^2) \cdot Q_0^2 \cdot g^2(x', k^2). \tag{41}$$

where $g(x,q^2) = xG(x,q^2)$ and P_G^G is the kernel of GLAP equation:

$$P_G^G = P'_{G'} - \delta(1-z) \int zP''_G(z)dz \tag{42}$$

$$P'_G(z) = 4N_c \cdot [\frac{1-z}{z} + \frac{z}{1-z+\Delta} + z(1-z)[\tag{43}$$

Here N_c is the number of colours; $\Delta \to 0$ is the infrared cutoff. Fist of all the GLR equation restores unitarity since the increase of the parton structure function is supressed by a nonlinear term which has negative sign in front. This sign appears as a result of the integration in the Feynman diagrams, but it has a simplest interpretation in terms of the balance equation for the number of partons in the parton cascade (see eq.(36)).

The coefficient in front of the second term consists of numerical factors that were calculated in perturbative QCD and a phenomenological parameter Q_0^2. This parameter [10] is related to the correlation radius of two gluons inside the hadron at $x \sim 1$. For purpose of estimating we assume that there are no either correlation between gluons in the hadron except for the fact that gluons are uniformly distributed in the disc of radius R_h. This assumption corresponds to the eikonal approximation in the calculation of Feynman diagrams. The correspondance between Q_0 and R_h was derived by Mueller and Qui [10] who found that $R_h^2 = 12 \cdot \frac{1}{Q_0^2}$.

Solution of the GLR equation.

Two years ago we knew only a semiclassical solution of the nonlinear GLR equation. In particular it was possible to find the equation for the critical line [3] on which the gluon density is constant

$$\phi(x,q^2) = \phi_0 = 31b\pi \frac{\sqrt{N_c^2-1}}{N_c} \cdot \frac{1}{Q_0^2} = \frac{31}{12} b\pi \frac{\sqrt{N_c^2-1}}{N_c}. \tag{44}$$

where the usual notation for running coupling QCD constant $\alpha_s = \frac{4\pi}{b\log(q^2/\Lambda^2)}$ is used. It was possible to solve this equation at large value of q^2 and the result turned out to

be

$$\log \frac{1}{x_{cr}(q^2)} = \frac{0.21b}{8N_c} \log^2 \frac{q^2}{\Lambda^2}. \tag{45}$$

This critical line possesses two remarkable properties:

1. To the right of this line, that is for $x > x_{cr}$, the theoretical accuracy of the GLR equation is such that for the gluons structure function is equal to

$$xG(x,q^2) = \{1 + O(\sqrt{\alpha_s})\} xG(x,q^2)_{GLR} \tag{46}$$

2. In the semiclassical approximation at very large value of q^2 and to the right of the critical line, the solution of the GLR equation is the same as the solution of the linear equation with the initial condition fixed on this line. This initial condition comes from the nonlinear equation and looks as follows :

$$xG(x,q^2) = xG(x_{cr},q^2) = \phi_0 q_0^2(x) = 0.4 \cdot R_h^2 q_0^2(x) \tag{47}$$

where R_h^2 is expressed in GeV^2. (see ref.[3] for more details).

Thus the critical line provides a real boundary between the transition region which is under theoretical control and the Regge domain. I would like to stress that the value of the structure function on the critical line is considerably smaller than the derived for $xG(x,q^2)$ from the unitarity constraint. $xG(x,q^2)$. At this point we can try to estimate the value of x at which the new physics could be reached. Even if we take $R_h = 1$ fm $= 5$ GeV the value of $xG(x,q^2)$ at $x = x_{cr}$ is expected to be

$$xG(x,q^2) \leq 10 q_0^2(x). \tag{48}$$

This is to be confronted with the estimates from the correct evolution equation. If, for instance, $xG(x,q^2 \sim 3(\frac{0.01}{x})^{\frac{1}{2}}$ as expected from the correct evolution equation at low x, then at $x = 10^{-4}$ one could predict $xG(x,q^2 \approx 30$. If this is the case, one might find rather spectacular effect in the HERA region for q^2 of the order of 3-4 GeV^2. If on the other hand R_h is replaced by the radius of constituent quark, that is $R_h = r_Q = 0.3$ fm $= 1,5$ GeV, the same effect would show up even at larger $x \sim 10^{-3}$.

These estimates are very close to that ones which were given by Mueller in his beautiful talk at the DESY low-x Workshop [11]. I hope, that the above example illustrates nicely how our estimates depend on our imagination on the nucleon structure

and how much the new experimental data are needed to unrovel the whole picture at low-x region.

Summariszing the situation in the transition region, as was two years ago I must say that we knew the semiclassical solution of the GLR equation and the equation for the critical line at large values of q^2 but we had neither a solution to the left of the critical line nor an equation for the latter at small (reasonable) values of q^2 (See Fig.1).

By now we have accumulated enough experience in solution of the GLR equation and know the main properties of such a solution in the whole deeply inelastic scattering region. This was made possible, mostly due to the hard work of Bartels, Shuler and Blumlein [12], Kwiecinski, Martin and Sutton [13], Kim and Ryskin [14, 15], Collins and Kwiecinski [14]. Let me summarize their results.

1. They found the numerical and even semiclassical analytical solution to the left of the critical line (see Fig.10). In this solution the parton density (ϕ) goes to the unitarity limit at very small x, in other words the parameter $W \to 1$ at $x \to 0$.

2. The existence of the critical line was confirmed and the exact form of the critical line was calculated. This form in the subasymptotical kinematical region turns out to be very different from the asymptotical one [12] but coincides with it at very large values of q^2.

3. The solution to the right of the critical line does not depend on the solution to the left of it. In particular, it does not depend on our hypothesis on the confinement of quarks and gluons, which is still an open question in QCD.

In principle there would be no needs to know the critical line, had the solution of the GLR equation been known in the whole kinematical region, but it is still of interest to know the border between the transition region and the Regge domain, which is given by this critical line. The solution to the left of critical line is very instructive in building our intuition about what may be happening in the Regge domain. This is why I shall discuss in the next section the properties of one of the possible solution. The discussion will be based on results that have not yet been published .

Anomalous dimension for GLR equation.

I would like to present here an analytical solution in a form which is very close to the solution of the linear GLAP equation. I will try to find this solution, by introducing

the anomalous dimension for moments of deep inelastic function in the usual way.

$$f(\omega,q^2) \;=\; \int_0^1 x^{(n-1)}(xG(x,q^2))dx \;=\; \int \exp(\omega\log\frac{1}{x})\cdot xG(x,q^2)d\log\frac{1}{x}, \tag{49}$$

$$f(\omega,q^2) \;=\; f(\omega)\cdot\exp(\gamma(\omega,r)r), \tag{50}$$

where $\omega = n-1$, $r = \log\frac{q^2}{\Lambda^2}$ and $\gamma(\omega,r)$ is the anomalous dimension. By substituting this form of solution in the GLR equation and restricting ourselves to the $\frac{1}{z}$ contribution to the kernel $P_G^G(z)$, we get the following equation

$$\{\omega\cdot\gamma(\omega,r) \;-\; \frac{N_c\alpha_s}{\pi}\}\, f(\omega)\exp(\gamma(\omega,r)r) \;=$$
$$=\; -\frac{9Q_0^2}{32q^2}\alpha_s^2\int f(\omega-\omega')f(\omega')\exp[(\gamma(\omega-\omega',r)+\gamma(\omega',r))r]\cdot\frac{d\omega'}{2\pi i}. \tag{51}$$

The integral on the r.h.s. of the equation can be obtained by using the steepest descent method. The value of the saddle point is $\omega' = \omega/2$. Finally, the equation can be reduced to the form

$$\{\omega\gamma(\omega,r) \;-\; \frac{N_c\alpha_s}{\pi}\}\cdot f(\omega)\cdot\exp[(\gamma(\omega,r)r] \;=$$
$$-\frac{9Q_0^2\cdot N_c\alpha_s^2}{32q^2\pi}\cdot\frac{f^2(\frac{\omega}{2})}{2\pi^{\frac{1}{2}}\sqrt{\gamma''(\omega/2)r}}\cdot\exp[2(\gamma(\frac{\omega}{2},r)r]. \tag{52}$$

When q^2 is large enough and ω is not very small, the r.h.s becomes negligible and we get the usual expression for the anomalous dimension in DLA (for small ω).

$$\gamma(\omega) \;=\; \gamma_{\rm LLA}(\omega) \;=\; \frac{N_c\alpha_s}{\pi\omega}. \tag{53}$$

However in the kinematical region where the r.h.si is of the order of the l.h.s. the equation for γ is the following:

$$\gamma(\omega,r) \;=\; -1 \;+\; 2\gamma(\frac{\omega}{2},r). \tag{54}$$

This functional equation has a very simple solution:

$$\gamma(\omega,r) \;=\; 1 \;+\; \gamma'(r)\omega. \tag{55}$$

Finally the solution for γ looks as follows:

1. for $\omega \geq \omega_{\rm cr}$

$$\gamma \;=\; \gamma_{\rm LLA}. \tag{56}$$

2. for $\omega \leq \omega_{cr}$

$$\gamma = \gamma_{n.p.} = 1 + \gamma'\omega. \tag{57}$$

The value of ω_{cr} can be determined from equation

$$\gamma_{LLA}(\omega_{cr}) = \gamma_{n.p.}(\omega_{cr}). \tag{58}$$

Using the explicit form for $\gamma_{n.p.}$ we obtain the following equation for ω_{cr}

$$\frac{\partial \gamma_{LLA}}{\partial \omega}|_{\omega=\omega_{cr}} = \frac{\gamma_{LLA}(\omega_{cr}) - 1}{\omega_{cr}}. \tag{59}$$

This is identical to the equation obtained for the critical line in the case of the GLAP kernel. Indeed, from this equation the value of ω_{cr} is

$$\omega_{cr} = \frac{N_c \alpha_s}{2\pi} \tag{60}$$

and

$$\gamma(\omega_{cr}) = \frac{1}{2}. \tag{61}$$

In the semiclassical approximation one can define the evolution paths in the $y = \log\frac{1}{x}, r = \log\frac{q^2}{\Lambda^2}$ plane which can then be calculated by using the saddle point method. The position of the saddle point is determined by (see refs. [3, 6])

$$y - y_0 = \frac{\partial \gamma}{\partial \omega} \cdot (r - r_0) \tag{62}$$

At $\omega = \omega_{cr}$ this equation desribes the critical line

$$y - y_0 = \frac{\pi}{4N_c\alpha_s} \cdot (r - r_0). \tag{63}$$

Within the semiclassical accuracy the structure function on this line is proportional to q^2, that is $xG(x, q^2) \propto q^2$.

To the left of the critical line, the GLR equation can be easily reduced to the following equation in the variable $z = \frac{4N_c\alpha_s}{\pi}(y - y_0) - (r - r_0)$:

$$-\frac{d^2\bar{\phi}(z)}{d^2z} + \frac{d\bar{\phi}(z)}{dz} = \frac{1}{4} \cdot \phi(z)[1 - \phi(z)]. \tag{64}$$

where

$$\bar{\phi} = \frac{\alpha_s}{\phi_0} \cdot \frac{xG(x, q^2)}{q^2} \tag{65}$$

and

$$\phi_0 = \frac{32\pi}{9n_c Q_0^2}. \tag{66}$$

The initial condition for this equation is

$$\frac{1}{\bar{\phi}(z=0)} \cdot \frac{d\bar{\phi}(z=0)}{dz} = \frac{1}{2}$$
$$\bar{\phi}(z=0) = \alpha_s.$$

We can easily find the semiclassical solution of this equation if we assume that

$$\frac{1}{\bar{\phi}(z)}\frac{d^2\bar{\phi}(z)}{d^2z} = (\frac{1}{\bar{\phi}(z)}\frac{d\bar{\phi}(z)}{dz})^2. \tag{67}$$

In this case

$$\bar{\phi}(z) = \frac{1}{[1 + (1 - \frac{1}{\sqrt{\alpha_s}}) \cdot \exp(-\frac{z}{4})]^2}, \tag{68}$$

and coincides with the solution, that has been found in ref.[14]. This solution can be used only in the vicinity of the critical line. I would like to postpone the detailed discussion of the solution of this equation and its generalization to the case of the FKL kernel and a running coupling constant to a separate publication.

Relation between renormalization group approach and the GLR equation.

Let me now discuss the relation between the standard approach to deep inelastic scattering, using the renormalization group equation and the Wilson operator product expansion. The understanding which I am going to suggest is a result of discussion with J. Bartels (see also ref. [10] where this question was discussed for the fist time).

In the standard approach the operator expansion is used for moments of deep inelastic structure function. It looks as follows, if we restrict ourselves only to the leading and next to leading twist contributions:

$$f(\omega, q^2) = f_1(\omega, q^2)\langle p|O_\omega^{(1)}|p\rangle + \frac{1}{q^2} \cdot f_2(\omega, q^2)\langle p|O_\omega^{(2)}|p\rangle. \tag{69}$$

where $O^{(1)}$ and $O^{(2)}$ are the operators of the leading and next to leading twists.

The next step is to use the renormalization group approach, in which since $f(\omega, q^2)$ a physical measurable quantity cannot depend on the renormalization point μ^2, the following holds

$$\mu^2 \frac{df(\omega, q^2)}{d\mu^2} = 0. \tag{70}$$

Thus the coefficient function f_1 and f_2 must satisfy the equation

$$\langle p|O^{(1)}_\omega|p\rangle(D-\gamma_1)f_1(\omega,\frac{q^2}{\mu^2},\alpha_s) \;+\; \frac{1}{q^2}\cdot\langle p|O^{(2)}_\omega|p\rangle(D-\gamma_2)f_2(\omega,\frac{q^2}{\mu^2},\alpha_s) \;=\; 0, \quad (71)$$

where

$$D \;=\; -\frac{\partial}{\partial\log q^2} \;+\; \beta(\alpha_s)\frac{\partial}{\partial\alpha_s}. \quad (72)$$

and $\gamma_1\,(\gamma_2)$ is the anomalous dimension of twist 1(2) operator.

At large values of q^2 contribution of the second term can be neglected and the usual GLAP equation for f_1 or for the deep inelastic structure function one obtains

$$(\,D \;-\; \gamma_1\,)\,f_1(\omega,\frac{q^2}{\mu^2},\alpha_s) \;=\; 0. \quad (73)$$

However if we assume that in the region of small ω the next twist contribution becomes comparable with the leading one, as happened with the solution of the GLR equation, eq. (73) does not determine the dependence of the deep inelastic structure function on q^2. It only provides some constraint on the two coefficient functions and additional information is needed to get the equation for deep inelastic structure function.In the GLR approach [3] the additional information was extracted from the analysis of Feynman diagrams, which lead to a relation between f_1 and f_2.

$$f_2(\omega,q^2) \;\propto -\frac{\alpha_s}{\omega}f_1^2(\frac{\omega}{2},q^2). \quad (74)$$

By now this relation has been confirmed by the calculation of the anomalous dimension of the next twist operator at $\omega\to 0$ [16]. It turns out that

$$\gamma_2 \;=\; 2\gamma_1(\frac{\omega}{2}). \quad (75)$$

However, even this relation is not sufficient to transform the equality into equation for the deep inelastic structure function. We need some correlation between the matrix elements of operators $O^{(1)}$ and $O^{(2)}$. We suggest the following ones

$$\langle p|O^{(2)}_\omega|p\rangle \;=\; \frac{1}{R_h^2}\cdot\langle p|O^{(1)}_{\frac{\omega}{2}}|p\rangle\langle p|O^{(1)}_{\frac{\omega}{2}}|p\rangle. \quad (76)$$

As we discussed, this assumption means that we neglect the correlation between gluons inside the hadron except for the fact that they are confined in the disc of radius R_h.

With this assumption we can easily get the GLR equation going back to x representation. The above discussion shows that the nonlinear equation takes into account

the high twist contribution in the region of small ω, where it is of the same order if not larger than the leading twist one.

From this consideration we can also conclude that the high twist contributions have to be large and negative since they provide the shadowing (screening) correction in deeply inelastic scattering even for the sea quark structure function (F_2^{sea}). I would like to draw your attention to the fact that Donnachie and Landshoff were the first to mention such a possibility [17].

Concluding this section I hope that I managed to convinced you that

1. We know by now the boundary of the transition region quite well.

2. We accumulated enough experience in the solution of the nonlinear GLR equation and are able to estimate the value and the main properties of shadowing (screening) corrections.

3. We are on the way to understand the relation between renormalization group approach and the direct analysis of Feynman diagrams which gives us the only reliable method to study the problem in the case when $\alpha_s \ll 1$ (in perturbative QCD).

Next steps.

Let me now discuss the next steps which I think could take us to further in the understanding of the deep inelastic scattering in the transition region.

1. At the moment we have a big gap between our understanding of the physical origin of the shadowing correction in terms of parton interactions and its description by the equation for the balance of the number of parton inside a parton cascade and the complicated analysis of Feyman diagrams which we still need to prove the GLR equation. I think, that we have to try to find a kinetic equation inside the parton cascade which will take into account both the emission and the recombination of partons.

2. We need to solve the nonlinear equation with the correct evolution equation for the linear part of the GLR equation to match the solution of this equation in the region of not very small x.

3. The most urgent and important problem is a consistent and detailed study of the high twists contributions. Let me summarize what we know at the moment about the high twists.

1). We know the evolution equation for high twist [18].

2). There were almost no attempts to solve these equations, but for Ali, Braun and Hiller [19]who calculated the anomalous dimension for the twist 3 operator, in other words they solved the evolution equation for $g_2(x,q^2)$ deep inelastic structure function and Levin, Ryskin and Shuvaev who found the behaviour of the anomalous dimension of the twist 4 operator at small ω [16], as has been already discussed .

3). There is experimental evidence for high twist contribution. The experimentalists use some factorization formula of the following type

$$F_2(x,q^2) \;=\; F_2^{\rm LLA}(x,q^2)\cdot\{\,1 \;+\; \frac{C}{q^2}\,\}. \qquad (77)$$

However I do not see any argument to support such an approach, on the contrary it was shown in [16] that the high twist structure function is rather proportional to F_2^2(LLA) than to F_2(LLA) as used in fitting of experimental data (at least at small x).

REGGE DOMAIN.

This kinematical region escapes any theoretical control. As I have mentioned there are plenty of ideas, but no well established theoretical results. These ideas cover a whole spectrum of different approaches, from the simplest attempt to solve the GLR equation in the Regge domain to very sophisticated imagination about confinement. The only good indication that we might have a chance to understand this domain in the future is the fact that the variety if ideas increases.

During this last year Bartels [20] developed in this domain a reggeon calculus which might help us in finding the main property of the behaviour of deep inelastic structure function or at least in studing the matching between the regge domain and the transition region.

Lipatov [21] suggested in this domain an effective theory for parton interaction whose lagrangian, unfortunately, is only a little bit simpler than that of QCD.

Among the contributed papers one finds a paper by Contogouris [22], who showed that all our difficulties in the Regge domain have an even more general ground than the explicit calculations in perturbative QCD.

I also firmly believe that Gribov's ideas about confinement of quarks and gluons [23] are very relevant to the situation in this region , especially near the border with the confinement region (see Fig.1).

Thus this region is free for any phenomenological hypothesis, but there is enough experience with some models [24, 25, 26, 27] to suggest the so called **saturation of the parton density** [3]. It implies that the parameter W, which we discussed before is equal to unity in the Regge domain, that is

$$W \;=\; \frac{\alpha_s}{q^2}\cdot\frac{xG(x,q^2)}{\pi R_h^2} \;=\; 1 \qquad (78)$$

at $q^2 \;\leq\; q_0^2(x)$. Saturation means that partons with an intrinsic size $r_G \sim \frac{1}{q_0(x)}$ are densely distributed in the hadron disc as shown in Fig. 11. Of course, we can not prove the saturation hypothesis, there are even some arguments [25] that W could be a smooth function of $\log\frac{1}{x}$. However, this hypothesis looks very transparent, since each gluon with transverse momentum (p_t) smaller that $q_0(x)$ should interact with a large number of gluons situated in an area of the order of $1/p_t^2$. Since the average colour charge of gluons in this area is very small such interaction is also very small. This fact leads to the suppression of the production of soft gluons. The emission of hard gluons with $p_t \gg q_0(x)$ is proportional to $\frac{q_0^2(x)}{p_t^2}$ and also small.

Perhaps the most important thing is that this hypothesis can be checked experimentally as the resulting behaviour of the deep inelastic structure function looks as shown in Fig.12. Saturation leads to $xG(x,q^2)\propto q^2$ in the Regge domain which induces a large scaling violation at low x.

Deeply inelastic scattering on nuclear target.

The nuclear targets gives the possibility to study a system of partons with high density, mostly because of the large number of nucleons inside the nucleus. In the case of a nucleus the interaction can take place not only between partons inside one nucleon, but also between partons from different nucleons. We can try to estimate how many nucleons may interact in a nucleus (A) through their partons. In the reference frame where the nucleus is fast the longitudinal distances between the nucleons in the nucleus becomes smaller by factor $\gamma \;=\; \frac{E}{M}$ because of Lorentz contraction. For a parton with momentum $q_l \;=\; xp_N\,\gamma$ is smaller by factor x . Two partons with transverse momentum q_t and a given x can interact only if the distance Δz between them is of the order of $\frac{1}{q_t}$ in

the frame in which they are at rest. In this case the wave functions of these two partons overlap spatially. We can estimate the distance between the nucleons that emitted those partons. In the lab. frame where the nucleus is at rest

$$\Delta z_{\rm lab} \;=\; \Delta z \cdot \exp(2\Delta y), \tag{79}$$

where Δy is the difference in rapidity between the nucleon and the parton,

$$\Delta y = \log(m/2p_N) - \log(q_t/2xp_N \;= \log(mx/q_t), \tag{80}$$

where m is the nucleon mass. Finally,

$$\Delta z_{\rm lab} \;=\; \frac{1}{mx} \;=\; \tau_{\rm lab} \;=\; \frac{1}{\Delta E} \;=\; \frac{2E}{q^2}. \tag{81}$$

Here τ is the typical proper lifetime of a parton. The number of nucleons (T) that can interact through their partons carrying a fraction x of their energy is equal to

$$T(b_t) \;=\; \int_{-\infty}^{\Delta z} \rho(b_t, z) dz, \tag{82}$$

where ρ is the nucleon density in the nucleus and z is an arbitrary point inside the nucleus at given impact parameter b_t. At small x all nucleons in a nucleus can take part in the interaction since $\Delta z \to \infty$.

Therefore the evolution equation in a nucleus should take into account the screening correction due to interaction of partons from different nucleons as well as from the same one. The only change in the the GLR equation is that for nuclear case the nonlinear part on has to be multiplied by factor

$$\{\, 1 \;+\; \frac{4\pi T(b_t, \Delta z)}{Q_0^2} \}. \tag{83}$$

(See ref.[24, 27, 28, 29] for details).

Such a small change in the evolution equation leads to a very different form of the critical line which describes the border between the transition and the Regge regions. Fig.13 shows this critical line for deeply inelastic scattering on both nuclei and nucleons. We can also illustrate the main difference between them using the unitarity constraint, at least qualitatively. Indeed for a nucleus target unitarity implies:

$$\sigma(\gamma^*, A) \;=\; A\sigma(\gamma^*, N) \;=\; \frac{\alpha_s}{q^2} \cdot A \cdot xG_N(x, q^2) \;\leq \pi R_A^2 \;=\; R_h^2 \cdot A^{\frac{2}{3}}. \tag{84}$$

Thus the saturation of unitarity in the nucleus case is expected much earlier than in the nucleon case even while the density of partons inside the nucleon (or the parameter W) is still small, namely

$$W_N \;=\; \frac{\alpha_s}{q^2} \cdot \frac{xG(x, q^2)}{\pi R_h^2} \;\leq\; A^{-\frac{1}{3}}. \tag{85}$$

This limit is overlayed with the dependence of the parton density (ϕ_N) behaviour versus q^2 (see Fig.13) the following observations can be made.

1. Since the critical line corresponds to large values of q^2, the typical transverse momentum of partons in the nucleus is larger than in the nucleon parton cascade. One can see in the figure that $q_0^2(N, x) \gg q_0^2(A, x)$.

2. The structure function of the nucleus approaches the saturation regime when the nucleon parton density is still small and can be calculated theoretically.

From Fig.13 we can also determine the kinematical region inside the "Regge" domain in which, we are able to apply perturbative QCD by developing a new approach. In this approach the relevant parameter to extract the essential Feynman diagrams is $\alpha_s A^{\frac{1}{3}} \sim 1$. The result obtained in this approach supports the hypothesis of parton density saturation [24].

I have mentioned only those problems in nuclear deeply inelastic scattering which are relevant to the study of the hadron structure function in "Regge" domain but, of course, much more to it. I am personally convinced that the theoretical and experimental study of deeply inelastic scattering on nuclei can clarify the physics of screening and be a testing grounds for our assumptions on the behaviour of deeply inelastic scattering in the "Regge" domain.

As has been pointed out by Badelek and Kwiecinski [30] even a detailed analysis of the structure function for deeply inelastic scattering on deuteron is of the great importance. Their paper contains a critical analysis of all approaches to the deeply inelastic scattering as well as an attempt to calculate the shadowing (screening) correction for this simple nucleus both, at large and small values of the photon virtuality (q^2).

The screening corrections for the deuteron can be described by a diagram that is shown in Fig.14. This diagram contains the "structure function " of the Pomeron, which although not quite well defined can be measured in diffractive dissociation on a proton target in deeply inelastic scattering on proton. With the formula derived in this

paper one should be able to calculate the deuteron screening correction in the future experimental data on diffractive dissociation.

Some numerical estimates are represented in Fig.15. The interesting result is that parton recombination inside one nucleon may turn out to be very important at small x ($x \sim 10^{-4}$) even for the lightest nucleus.

PHENOMENOLOGY.

I would like to restrict myself to a discussion of the estimates of the size of screening corrections in deeply inelastic scattering and of the kinematical borders between different regions (see Fig.1). As could be infered from the GLR equation the value of screening correction depends crucially on the value of a radius R_h which enters into the nonlinear term of the equation. Unfortunately, we are not able to estimate R_h from theory and we have to rely on our experience with models for the structure of hadrons, on common sense and on the available experimental data on deeply inelastic scattering or on hadron interaction. There are basically two estimates for the value of R_h, one pessimistic and one optimistic.

1. Pessimistic estimates.

The most natural assumption is that that R_h is equal to the radius of the proton ($R_N \sim 1\,Fm$). That implies that gluons are distributed uniformly inside the whole hadron disc, as shown in Fig.16a. In this case the screening correction turns out to be very small, at least at $x > 10^{-4}$. The best presentation of this approach can be found in the Mueller's talk from the DESY low-x Workshop [11].

2. Optimistic approach.

In this approach we assume that gluons inside a hadron are confined within disc with a radius smaller than the size of the hadron (see Fig.16 b) [27]. This picture of a hadron is a reminder of the old constituent quark model, which described nicely the main properties of hadrons and their interactions. Such a picture leads to quite large value of the screening correction, which depends crucially on the value of the radius of the "hot spots" (constituent quark) inside the hadron. From hadron production experiments we have estimated that R_Q is of the order of 0.2 Fm [27], while the traditional value of R_Q

for constituent quarks is of the order of $R_Q = 0.4$ Fm, as used by Kwiecinski, Martin and Sutton [13].

The difference between this two approaches can be seen in Fig.17 taken from the KMS paper [13]. If the optimistic pictureis true we have a good chance to observe the screening correction at HERA experiments.

Let me to draw your attention to the fact that these two approaches can be differenciated experimentally, at least in principle.

In the first one the value of the screening corrections depend on the radius of the hadron and is different for different hadrons. Thus the parton distributions should be different for different hadrons, if we take into account the nonlinear term in the GLR equation. That means, that for example the screening correction to the parton distribution inside the pion should be larger than for the nucleon.

In the second one the sreening corrections are the same for all hadrons. Only if this approach is correct we can use the same parton distributions for the deeply inelastic scattering and for the analysis of jet or hadron production at high energy hadron-hadron collisions.

The best reaction to observe this difference, is the $\gamma^* p$ collision, when the photon virtuality (q^2) is small enough ($q^2 < q_0^2(x)$). We can use the high p_t hadron or jet production to measure the photon structure function. There are different estimates for the hadronic part of the photon structure function depending on the approaches while for the so called point-like part both approaches give the same scale for screening which corresponds to $R_h \propto \frac{1}{q^2}$. You should keep in mind that the radius of the pion is two times smaller than that of the proton. Thus the screening correction to the hadronic part of the photon structure function are expected of the same size as the MRS estimates for $R_h = 0.4Fm$.

Let me now discuss one qualitative argument in support of the "hot spot" picture of hadrons, which is quite convincing. In the parton model we calculate the cross section for jet production by factorization formula

$$\frac{d\sigma^{jet}}{dk_t^2} = \int dx_1 dx_2 x_1 G(x_1, k_t^2) x_2 G(x_2, k_t^2) \hat{\sigma}(GG \to jet + jet), \qquad (86)$$

where the notation should be clear from Fig.18. But in QCD the hard cross section is

roportional to

$$\hat{\sigma} \propto \frac{\alpha_s}{k_t^4}. \tag{87}$$

Thus our cross section diverges at low k_t and in order to calculate the jet contribution o the total inclusive cross section we have to introduce some minimal value of k_t to egularize the integration over k_t ($k_t > k_{cutoff}$). Of course, this contribution has to be maller than total inclusive cross section. However, even if we assume that all hadrons riginate from the jet decay, the value of the k_{cutoff} is found to be large and growing with energy. Indeed, $k_{cutoff} \approx 1$ GeV at ISR energies, 2.5 GeV at $Sp\bar{p}S$ energies, 3.5 GeV at Tevatron energy and might even be 5 GeV at cosmic ray energies. A reasonable xplanation of this fact is provided by screening effects which prevent the increase of he total cross section for jet production at small transverse momenta ($k_t \leq q_0(x)$). The natural suggestion would be identify k_{cutoff} with the the critical line $q_0(x)$. In fact he phenomenological formula for critical line

$$q_0^2(x) = Q_0^2 + \Lambda^2 \cdot \exp 3.56\sqrt{\log \frac{x_0}{x}}, \tag{88}$$

with $Q_0^2 = 2$ GeV^2, $\Lambda = 52$ MeV, $x_0 = \frac{1}{3}$ that extracted from the description of experimental data on hadron production at high energies (see ref.[27]), leads to the value of $q_0(x)$ very close to what is needed, with reservation that in the above formula only the form and the coefficient in exponent can be guaranteed.

Smooth description of $\sigma_{tot}(\gamma^* p)$ from deeply inelastic scattering to real photoproduction.

In an attempt to explore whether the Regge language could be used also in the domain of deeply inelastic scattering, the ALLM collaboration [31] has come up with a smooth parametrization of the photoabsorption cross section $\sigma(\gamma^* p)$, in the whole of the kinematical explored by the data, including the real photoproduction cross section. The parametrization is based on a new kinematical variable,

$$x_P = \{ 1 + \frac{W^2 - m_p^2}{Q^2 + m_p^2} \} \tag{89}$$

defined in such a way that at $Q^2 = 0$ and in the limit of high W^2 it becomes proportional to the energy and tends to x_B for Q^2 larger than a certain mass scale m_p^2 to be determined from a fit to the data. The parametrization describes well: both the real

photoproduction cross section and the electromagnetic structure function as can be seen in Fig.19.

The interesting observations which can be drown from this purely phenomenological approach are the following:

1. It is possible to get a good description of all experimental data (see Fig.19).

2. The higher twist corrections are large and negative, since the value of m_p^2 turns out to be about 10 GeV^2 in this parametrization.

3. There seems to be some transition region for $Q^2 = 1 - 10 GeV^2$, where the total cross section depends very weakly on Q^2 and its value is about 5 times smaller than the value of the total cross section for real photoproduction (see Fig.20). This observation could support the hypothesis that hadrons consist of constituent quarks or hot spot, with their radius in 2-3 times smaller than that of a hadron .

I think that such a parametrization can be used to specify the initial condition for the evolution equation to be solved both in the $\ln q^2$ direction for which we can need $F_2(x)$ at $q^2 \approx 4 - 8$ GeV^2 and in the $\ln x$ direction using $F_2(q^2)$ at $x = 10^{-1} - 10^{-2}$.

HERA PHYSICS.

In this section I am going to discuss what new phenomena we can expect at low-x region at HERA and how to detect them. Now it is very fashionable to present each new regime as some phase transition. We can do the same for deeply inelastic scattering (see Fig.21).

1. In the "standard" evolution region our system of partons can be considered to be a perfect gas since we neglect an interaction between them and only take into account emission of partons in the evolution equation.

2. In the transition region such interactions are taken into account, but only when they are sufficiently weak. Here the parton cascade is very similar to Van der Waals gas. This analogy explains why it is really important to describe this transition region theoretically. Indeed, the Van der Waals equation provides us with the qualitative understanding of all phenomena in liquids and even provides a semiquantative description for many of them.

3. In the "Regge" domain the parton cascade behaves more like the quark-gluon

liquid than gas. The density of partons is large here, but correlations or more precisely interactions between partons is still sufficiently weak due to smallness of coupling constant QCD (α_s) in this domain.

The most interesting problem for HERA is to penetrate inside the "Regge" domain and study the quark-gluon liquid. However the fist step for HERA is, of course, to investigate the transition region and to observe the deviation from the linear evolution equation, which would indicate a substantial screening (shadowing) correction. Estimates which have been made (see ref.[13, 14]) show that the transition region could be measured at HERA , at least whithin the context of the picture of proton with two radii. In Fig.22, which I took from ref.[14] you see the most optimistic estimates for three regions in the HERA map.

Let me now review some of the main ideas how to look at the transition and even the "Regge" regions at HERA. Most of these are now beeing discussed at HERA Working Groups to prepare more reliable proposals for coming experiments.

1. $\mathbf{F_2(x,q^2), F_l(x,q^2)}$.

The fist idea is trivial, namely to measure the behaviour of the deep inelastic structure function and compare its behaviour with theoretical expectations at small x. For this purpose we need reliable predictions for the structure function. It means that we should overcome at least two problems:

1.To solve the correct evolution equation at low x. Fortunately, experience that we have accumulated in solution of the correct equation showed us that we can use the GLAP equation at HERA within accuracy 5% [5,6,7] for all initial conditions. However, you should keep in mind that the gluon structure function depends crucially on the equation that one used at $x < 10^{-3}$ for sufficiently small $q^2 \approx 10$ GeV^2 [7].

2. To specify the initial condition for evolution equation. One of the serious problems at HERA at low x, is the fact that we do not know the initial conditions for gluon structure function in this kinematical region (see HERA map in Fig.22). In the usual procedure for solving the GLAP equation one has to specify the value of structure function at fixed and small $q^2 = q_0^2 \approx 3 - 4$ GeV^2. Unfortunately, as shown in Fig.22, a constant q^2 line overlaps the measurement region in a very limitted x- range. Therefore, the GLAP equation which governs this evolution cannot be tested directly and provide us with the basis to detect new phenomena in HERA region. We can discuss

the solution only in context of a specific parametrization chosen at $q^2 = q_0^2$.

The main suggestion of how to avoid this difficulty is to solve the GLAP equation in HERA region. Krasny, Levin and Ryskin gave the modification of GLAP equation specifically suited for the HERA strip [32] for which we need to stipulate the inital condition on the line with fixed $y = \frac{q^2}{xs_{ep}} = y_{max}$. However, experimentalists have to measure two functions at $y = y_{max}$, namely $F_2(x,q^2)$ and $dF_2(x,q^2)/d\log q^2$.

After solving the GLAP equation in the HERA region we will be able to get theoretical prediction for evolution to smaller y. We can then compare this solution with experimental data, and extract information about QCD parameters such as coupling constant α_s or Λ QCD and to see the deviation from the GLAP equation due to screening corrections.

The next question is at what particular observable can we see the largest contribution originated from screening corrections. The solution of GLR equation, shows that the largest contribution should be in the slope of structure function (see ref.[3] for details). We gave the simple formula to estimate the slope with screening corrections [32], namely

$$\Delta\gamma \;=\; \gamma_{exp} \;-\; \gamma_{QCD} \;=\; -\,\gamma_{exp}\cdot W(x,q^2), \tag{90}$$

where

$$\gamma \;=\; \frac{1}{F_2(x,q^2)}\cdot\frac{\partial F_2(x,q^2)}{\partial\xi} \;\; and \;\; \xi \;=\; \log\log(q^2/\Lambda^2). \tag{91}$$

From the above expression we can measure the value W which is equal to

$$W \;=\; \frac{27\pi\alpha_s(q^2)}{16q^2R^2}\cdot xG(x,q^2). \tag{92}$$

The value of W could be extracted from experimental data but of course after that there still remains a lot of work, to understand the value of R^2 and $xG(x,q^2)$. However this is a job more for the theoriticians than for experimentalists. Using KMS estimates for W we can evaluate $\Delta\gamma$. It turns out that $\Delta\gamma$ is equal to 1.3 γ_{exp} and 0.6 γ_{exp} at $x = 10^{-4}$ and $x = 10^{-3}$,respectively, at $q^2 = 4$ GeV^2. For $q^2 = 20$ GeV^2 at the same value of x we have $0.5\gamma_{exp}$ and $0.1\gamma_{exp}$. These large numbers were calculated in the model with $R^2 = 0.4\,Fm\,(2GeV^{-1})$.

Thus, I believe that HERA might measure the screening correction, if the experimental accuracy will be high enough to measure $\Delta\gamma$ accordingly to the above estimates. However, we have still a very important problem that is to study the stability of the

solution of evolution equation in the HERA strip, and to specify the experimental accuracy necessary in measuring the deep inelastic structure function and its derivative on the line with $y = y_{max}$.

2.Direct measurement of $xG(x,q^2)$.

Of course, it will be even more natural to directly measure the gluon structure function at HERA. In this case we could calculate W and this measurement in some sense is complementary to F_2 measurement. For this purpose we could use the heavy quark production, namely the reaction of the following type (see Fig.23)

$$\gamma^* p \rightarrow c\bar{c}(b\bar{b}) + X. \tag{93}$$

The cross section for this reaction has been discussed in ref.[33] in early days of HERA project and now Webber [7] has again estimated the cross section of this reaction using the correct evolution equation and all novel features which should be taken into account in the region of small x [34]. The result is that the value of the total cross section for charm and beauty production is large enough,namely of the order of $1\mu b$ and 8 nb, respectively, in the HERA kinematic region. So we can attempt to measure $xG(x,q^2)$ in charm production at $x \geq 10^{-4}$ and in beauty production at $x \geq 10^{-3}$, but of course only at definite value of q^2 , namely $q^2 = 4m_Q^2$, as a function of x.

3. Diffraction dissociation of virtual photon.

Ryskin [35] proposed to measure the diffraction dissociation of photon in the reaction at HERA (see Fig.24)

$$\gamma^* p \rightarrow X + p. \tag{94}$$

The great advantage of this reaction, is the fact that the cross section is proportional to $(xG(x,q^2))^2$. The theoretical prediction for diffraction dissociation, is very sensitive to the value of the gluon structure function and its behaviour at small x. Indeed,

$$\frac{M^2 d\sigma}{dt dM^2} \propto \frac{\alpha_{em}}{Q^2} \cdot \int D(\frac{x}{x_k}, Q^2, k^2)[x_k G(x_k, k^2)\frac{\alpha_s}{k_t^2}]^2 \frac{dx_k}{x_k} d^2k_t. \tag{95}$$

The notation is explained in Fig.24.

Our cross section is infrared unstable, since $\frac{d\sigma^{DD}}{dtdM^2} \propto \int \frac{d^2k_t}{k_t^4}$ and the region of small k_t really defines the value of the cross section. So we expect the cross section to be of the order of $\frac{1}{\Lambda^2}$ where Λ is infrared cut off, i.e large enough ($\sim$ 2-10 nb [36]). However, if you take into account screening corrections, the role of cutoff played by $k_t = q_0(x)$

than the cross section turns out to be two orders of magnitude smaller than the naive estimates [35], namely 0.01 nb at $Q^2 = 30 - 100$ GeV^2, $M^2 = 300 - 1000$ GeV^2, $x_k = (0.3 - 1)10^{-3}$.

I would like to draw your attention to the fact that the measurement of this process is very important, since the scale of the screening correction is proportional to the value of the cross section of the diffraction dissociation integrated over momentum transfer t (see Fig.24).

4. "Hot spot" hunting.

Mueller suggested the beautiful idea of an experiment where one can measure the absorption in a situation where it should be strong [11]. Let us consider the inclusive production of gluon jet with transverse momentum k_t, which is very close to q, and with fraction of energy as close to one as possible so as to provide a small value of x_B/x_k (see Fig.25). In this case, the scale of the absorption correction is determinated by the size of the "hot spot", namely $R \propto \frac{1}{k_t}$ and which should be large. We can calculate the basic contribution since virtualities q^2 and k_t^2 both are large. In this case of course we have to use LL(x)A of the perturbative QCD (or the FKL equation but with running coupling constant α_s). There is a problem in that HERA has very strong experimental limitation on the value x_k, so it is not completely clear yet this nice idea could be realized at HERA.

Let me note that in this experiment we could also observe what will happen in the event of large gluon density, and answer the question whether there is or whether there is no the saturation of the gluon density. However, in this experiment we cannot distingvish between two situations: 1)"hot spot" exists as a rare fluctuation in our hadron, in which gluons are distributed uniformly on the average or 2) "hot spots" as the typical structure of a hadron as was suggested in the model with two radii.

5. Structure of typical inelastic event in the deeply inelastic scattering.

As we have discussed, the trajectory method allows us to calculate the structure of typical inelastic event in deeply inelastic scattering. Namely, we can predict the fraction of energy for our parton, as a function of its transverse momentum for those partons whose emission gives the dominant contribution to the structure function. So finally, we should see some oscilations for energy flow as shown in Fig.26 and we can then reconstruct the trajectory from the direct measurement [37]. Unfortunately, the

dispersion around trajectory is large ($\Delta \log k_{it}^2 \sim 2-3$), so that more work with Monte Carlo simulation of the parton (hadron) final states in deep inelastic process is needed in order to gauge how reliable these kind of experiments are. Even if it is not successful it is very important to realize that our evolution equation contains direct information about the structure of the inelastic event which could be measured.

6. Two particle correlations.

I firmly believe that one of the best ways to measure the value of the absorption (screening) correction is the usual correlation function analysis of the secondary hadron production [37]. This analysis was discussed in detail for multiparticle production in hadron-hadron and collisions and hadron - nucleus collisions [38] in the reggeon approach. The main idea of the analysis is that the pomeron is a collection of uncorrelated particles. Many years ago we started with a hypothesis. In deeply inelastic scattering we know what is the pomeron. It is our parton cascade which we are able to calculate. It turns out, that correlations in rapidity for emitted partons is negligible at low x [38]. So the main idea of the experiment is to measure the correlation function for two hadrons

$$R(y_1,y_2) \;=\; \frac{\frac{1}{\sigma_{tot}}\cdot\frac{d\sigma}{dy_1\,dy_2}}{\{\frac{1}{\sigma_{tot}}\cdot\frac{d\sigma}{dy_1}\}\{\frac{1}{\sigma_{tot}}\cdot\frac{d\sigma}{dy_2}\}} \;-\; 1. \tag{96}$$

We can write the result of measurement in the form:

$$R(y_1,y_2) \;=\; LR \;+\; SR\exp(-\frac{\Delta y}{\Delta_{SR}}). \tag{97}$$

The fist term does not depend on Δy and its value is directly correlated with screening corrections in the evolution equation. At HERA we expect LR is of the order of 50%. The second term is the short range correlations which depend on hadronization stage, as well as on the decay of produced jet. Now we can only estimate the value of the correlation length Δ_{SR} which is of the order of 2. The ideal behaviour for $R(y_1,y_2)$ is given in Fig.27, however, what the correlations will look like at HERA is still open question .

7. Dissociation of the target proton.

Let me discuss one more interesting exclusive process in deeply inelastic scattering, namely, reaction

$$\gamma^* \, p \to \Psi(\rho^0 ....) \;+\; X(M). \tag{98}$$

The cross section for this reaction can be written in the form:

$$M^2\frac{d\sigma}{dM^2dt} \;=\; \int \phi^2(y-y',Q_t,k^2)\cdot\alpha_s^2(k^2)\cdot G_{3P}\phi(y',k^2,q_0^2) \tag{99}$$

where t $=Q_t^2$. The most interesting factor here is the t-dependence. Indeed, $\phi(y-y',Q_t^2,k^2)$ depends on t, only if —t— $\geq q_0^2(x') = q_0^2(M^2/s)$. For smaller t our amplitude is really independent of t. Of course this prediction is only correct when we reach the saturation region.

Unfortunately we have had no numerical estimates of the cross section, in spite of the fact that we have all theoretical ingredients to perform the necessary calculations.

8. Jet (hadron) production with large transverse momentum.

Let us consider the jet (hadron) production in deeply inelastic scattering with transverse momentum large that q^2 ($k_t > q$). With x_{jet} as large as possible, we could calculate the screening correction in this process, since they are big enough, and have a scale of the order of $R^2 \propto 1/q^2$, as I discussed before. In the case when $k_{(jet)t} \approx q$ we have the same situation as in the Mueller reaction. In this case I see two advantages:

1. The absorption (screening) correction is under theoretical control for $k_t > q$.

2. In the case when $k_t \approx q$ we have better chance to catch this jet or hadron at HERA since it is emitted at a larger angle.

Concluding this section I would like to mention, that we have a lot of theoretical ideas of how to explore the region where new physics may appear, but still we need more theoretical work,to develop the tools from these ideas for HERA experiments. I will be happy if this talk will stimulate theoretical activity in this field of high energy physics. I have to repeat once more, that we are discussing not only the deeply inelastic process that is interesting , but also that we are not able to discuss the hadron collisions without understanding of the low-x behaviour of deeply inelastic scattering.

CONCLUSIONS.

The main conclusion looks as follows:

At the moment we have reached the understanding of the basical problems in the deeply inelastic scattering at low x and can formulate the nearest steps to solve them.

Let me list here the most important problems that are needed to solve.

1.Solution of the correct evolution equation in the $\ln x$ direction.

Such a solution may allow to specify the initial condition for the GLAP equation and to give reliable prediction for hard process in hadron-hadron collisions.

2. Systematical theoretical study of multipartical production in the deeply inelastic process.

At the moment there are only several theoretical papers devoted to this problem [3,27,39] while the coming HERA experiment will provide a lot of information on inclusive production in the deeply inelastic scattering. To illustrate how important namely theoretical study I would like to draw attention to contributed paper of Chay, S.Ellis and Stirling [40] in which the very interesting correlation between incoming electron and outgoing hadron was predicted.It should be stressed that this correlation was completely missed in any Monte Carlo simulation for the deeply inelastic process.

3. Consistent calculation of the next order correction to correct evolution equation in the deeply inelastic scattering as well as to inclusive and to exclusive processes.

Only such a calculation might provide the predictions which are independent of the renormalization scale and answer the questions what is the scale for the running coupling constant of QCD or what is the value of the cross section for jet or heavy quark production (so called K-factor).

4. Systematic study of the higher twists contribution to the deep inelastic structure function.

This project should contain the solution of the evolution equation for the higher twist structure function and also the study of different models of the hadron structure to specify the form of the matrix elements of the operators of the higher twists.

5.Development of leading log approximation for amplitude of the deeply inelastic scattering not only at the zero transferred momentum (t) but at $t \neq 0$.

As has been mentioned before, many processes ,for instance diffraction dissociation, depend on such amplitudes. Thus more theoretical information is needed to drive to some definite conclusions about these exclusive processes.

6. The influence of confinement forces on the low-x behaviour of the structure function is still open question.

7. We need transparent physical language to discuss all phenomena in the saturation region where we cannot apply the parton picture. I hope, that we can guess this language studing the kinetic equation for partons inside the parton cascade in the transition

region.

To compensate too theoretical presentation I am trying to describe the situation in Fig.29 which does not need any comments. Thus the today situation in the deeply inelastic scattering looks as follows. Experimentalist are doing the best to get the drop of the quark-gluon liquid at HERA, while theoreticians have started to prepare the glass to catch it from the boilling ideas.

Acknowledgements.

I am very grateful to H. Abramovich, J. Bartels, A. Gotsman, J. Feltesse, W. Krasny and M. Ryskin for useful discussions on the subject. I would like to acknowledge the hospitality extended to me at DESY Theory Group where this talk was prepared.

References

[1] V. N. Gribov, L. N. Lipatov: Sov.J.Nucl.Phys.15 (1972) 438.
L. N. Lipatov: Yad. Fiz. 20 (1974) 181.
Yu.L.Dokshitzer: Sov.Phys JETP 46 (1977) 641.
G. Altarelli, G. Parisi: Nucl.Phys. B126 (1977) 298.

[2] E. A. Kuraev, L. N. Lipatov and V. S. Fadin: Sov. Phys. JETP 45 (1977) 199.
Ya. Ya. Balitskii and L. N. Lipatov: Sov. J. Nucl. Phys. 28 (1978) 822.

[3] L. V. Gribov, E. M. Levin and M. G. Ryskin: Phys.Rep. 100 (1983) 1.

[4] M. Ciafaloni: Nucl.Phys. B 296 (1987) 249.
S. Catani, F. Fiorani and G. Marchesini: Nucl.Phys B 336 (1990)18.
S. Catani, F. Fiorani, G. Marchesini and G. Oriani: Nucl.Phys B (to appear).
G.Marchesini: Erice Eloisatron Workshop in perturbative QCD (June 1991)L.Cifarelli and Y. Dokshitzer ed. (World Scientific to appear).

[5] G. Marchesini and B. Webber: Nucl.Phys. B 349 (1991)1617.

[6] E. M. Levin, G. Marchesini, M. G. Ryskin and B. Webber: Nucl.Phys. B 357 (19991) 167.

[7] B Webber: talk at HERA Working Group meeting (Sept 1991).

[8] M. Gluck, E. Reya and A. Vogt: Nucl.Phys.B (Proc.Suppl.) 18C (1990) 49 and references therein.

[9] Wu-Ki Tung: Nucl.Phys. B 315 (1989) 378 Nucl.Phys. B (Proc. Suppl.) 18C (1990) 55.

[10] A. H. Mueller and J.Qiu: Nucl.Phys. B268 (1986) 427

[11] A. H. Mueller: Nucl.Phys.B (Proc.Suppl.) 18C (1990) 133.

[12] J. Bartels, J. Blumlein and G. Shuler: Z.Phys.C 50 (1991) 91.

[13] J. Kwiecinski, A. D. Martin and P. J. Sutton: DTP/91/10 March 1991 . Contributed paper 452.

[14] J. C. Collins and J. Kwiecinski: Nucl. Phys. B 335 (1990) 89.
M. G . Ryskin: Yad.Fiz. 53 (1991) 1077.

[15] V. T. Kim and M. G. Ryskin: DESY - 91 - 064 Sept. 1991.

[16] E. M. Levin, M. G. Ryskin and A. Shuvaev: Yad.Fiz.(in print).

[17] A. Donnachie. P. V. Landshoff: Nucl.Phys. B 224 (1984) 322.
P. V. Landshoff: Nucl.Phys B(Proc.Suppl) 18C (1990)211.

[18] A. P. Bukhvostov, G. V. Frolov, L. N. Lipatov and E. A. Kuraev: Nucl.Phys. B 258 (1985) 601.

[19] A. Ali, V. M. Braun,G. Hiller: DESY 91-041 May 1991, contributed paper 341.

[20] J. Bartels: DESY - 91 074 July 1991.

[21] L. N. Lipatov: IPNO/TH 91-21, April 1991.

[22] A. P. Contogouris: Contributed paper 21.

[23] V. N. Gribov: LU TP 91-7 March 1991.

[24] E. M. Levin, M. G. Ryskin: Sov.J.Nucl.Phys.41 (1985) 300,Nucl.Phys . B 304 (1988) 805.

[25] A. H. Mueller: Nucl.Phys B 335 (1990) 115, Nucl.Phys B 317 (1989) 573, Nucl.Phys. B307 (1988) 34.

[26] J. C. Collins and J. Kwiecinski: Nucl.Phys B 335 (1990) 89, Nucl.Phys. B 316 (1989) 307.

[27] E. M. Levin and M. G. Ryskin: Phys.Rep. 189 (1990) 267.

[28] A. H. Mueller and J. Qiu: Nucl.Phys.B 268 (1986) 427.
J. Qiu: Nucl.Phys B 291 (1987) 746.

[29] J. Kwiecinski: Z.Phys. C29 (1985) 147, 561.

[30] B. Badelek and J. Kwiecinski: IFD/3/1991,contributed paper 257.

[31] H. Abramowicz, E. M. Levin, A. Levy and U. Maor: DESY - 91 - 068,June 1991.

[32] M. W. Krasny, E. M. Levin and M. G. Ryskin: DESY 91-073,July 1991.

[33] A. Ali et al.: DESY HERA Workshop 1987 p. 395 (QCD.161:H15:1987).

[34] E. M. Levin, M. G. Ryskin, Y. M. Shabelski and A. G. Shuvaev: LNPI-1643 Oct.1990.
S. Catani, M. Ciafaloni and F. Hautmann: Cavendish -HEP-90-27 Dec. 1990.
J. C. Collins and R. K. Ellis: FERMILAB-Pub-91/22-T Jan.1991.

[35] M. G. Ryskin: Yad. Fiz.52 (1990) 828, DESY 90-050 May 1990.

[36] G. Ingelmann and P.E. Shlein: Phys.Lett.152B (1985) 256.

[37] E. M. Levin: LPTHE Orsay 91/02 Jan. 1991.

[38] E. M. Levin and M. G. Ryskin: Sov. J. Nycl. Phys. 21 (1975) 206.
A. Capella and A. Krzywicki: Phys. Rev. D18 (1978) 4120.

[39] L. V. Gribov and M. G. Ryskin: LNPI-865 June 1983.
L. V. Gribov, Yu. L. Dokhitzer, S. I. Troyan and V. A. Khoze: Sov.Phys. JETP 88 (1988) 1303.

[40] J. Chay, S. D. Ellis and W. J. Stirling: DOE/ER/40423-28, contributed paper 337.

Figure Captions.

Fig. 1 -: Kinematical subregions for the deeply inelastic scattering.

Fig. 2 -: The "standard" evolution region and the typical branching process.

Fig. 3 -: The next order corrections to the typical "ladder" diagram.

Fig. 4 -: The Monte Carlo solution of correct evolution equation [5] .

Fig. 5 -: a) Trajectories : full line for the correct evolution equation, dashed lines for the GLAP equation. b) Dispersion around trajectories.

Fig. 6 -: The general structure of the parton cascade for the fast hadron.

Fig. 7 -: The emission and annihilation of partons in the parton cascade.

Fig. 8 -: The coherence in the "ladder" diagram.

Fig. 9 -: The "fan" diagrams.

Fig.10 -: The situation in the transition region.

Fig. 11 -: The parton distribution in the transverse plane in the hypothesis of the parton density saturation.

Fig. 12 -: The behaviour of $xG(x,q^2)$ versus q^2 at fixed x.

Fig. 13 -: The critical line for the deeply inelastic scattering on nuclear target.

Fig. 14 -: The Feynman diagram for the screening correction on the deuteron.

Fig. 15 -: The value of the screening correction for the deuteron for $Q^2 = 10GeV^2$. Long dashed curve shows unevolved δF_{2D} while the others show the effects of QCD evolution starting from $Q^2 = 4GeV^2$. Continuous line corresponds the evolution without parton recombination. The dotted curve results for the gluon distribution with singular behaviour $x^{-1/2}$ and shadowing effects. The figure is taken from ref.[30].

Fig. 16 -: The models for the parton distribution at $x \sim 1$ in the hadron in pessimistic (a) and optimistic (b) estimates of the value of the screening correction in the GLR equation.

Fig. 17 -: The MRS estimates [13] for the ratio of the nonlinear term to the linear one in the GLR equation.

Fig. 18 -: The hard process in the parton model.

Fig. 19 -: The comparison of the ALLM parameterization with the experimental data [31].

Fig. 20 -: The transition region for $\sigma(\gamma^* p)$ in the ALLM parametrization [31] .

Fig. 21 -: The phase transition plot for deeply inelastic scattering.

Fig. 22 -: The subregions of the deeply inelastic scattering in HERA map (the most optimistic estimates [15]).

Fig. 23 -: The heavy quark production in the deeply inelastic scattering.

Fig. 24 -: The photon diffraction dissociation in the deeply inelastic scattering.

Fig. 25 -: The "hot spot" hunting experiment.

Fig. 26 -: The energy flow for typical inelastic event in the deeply inelastic scattering.

Fig. 27 -: The behaviour of the two particle rapidity correlation function in the deeply inelastic scattering.

Fig. 28 -: The dissociation of the target proton in the deeply inelastic process.

Fig. 29 -: The picture of the deeply inelastic scattering.

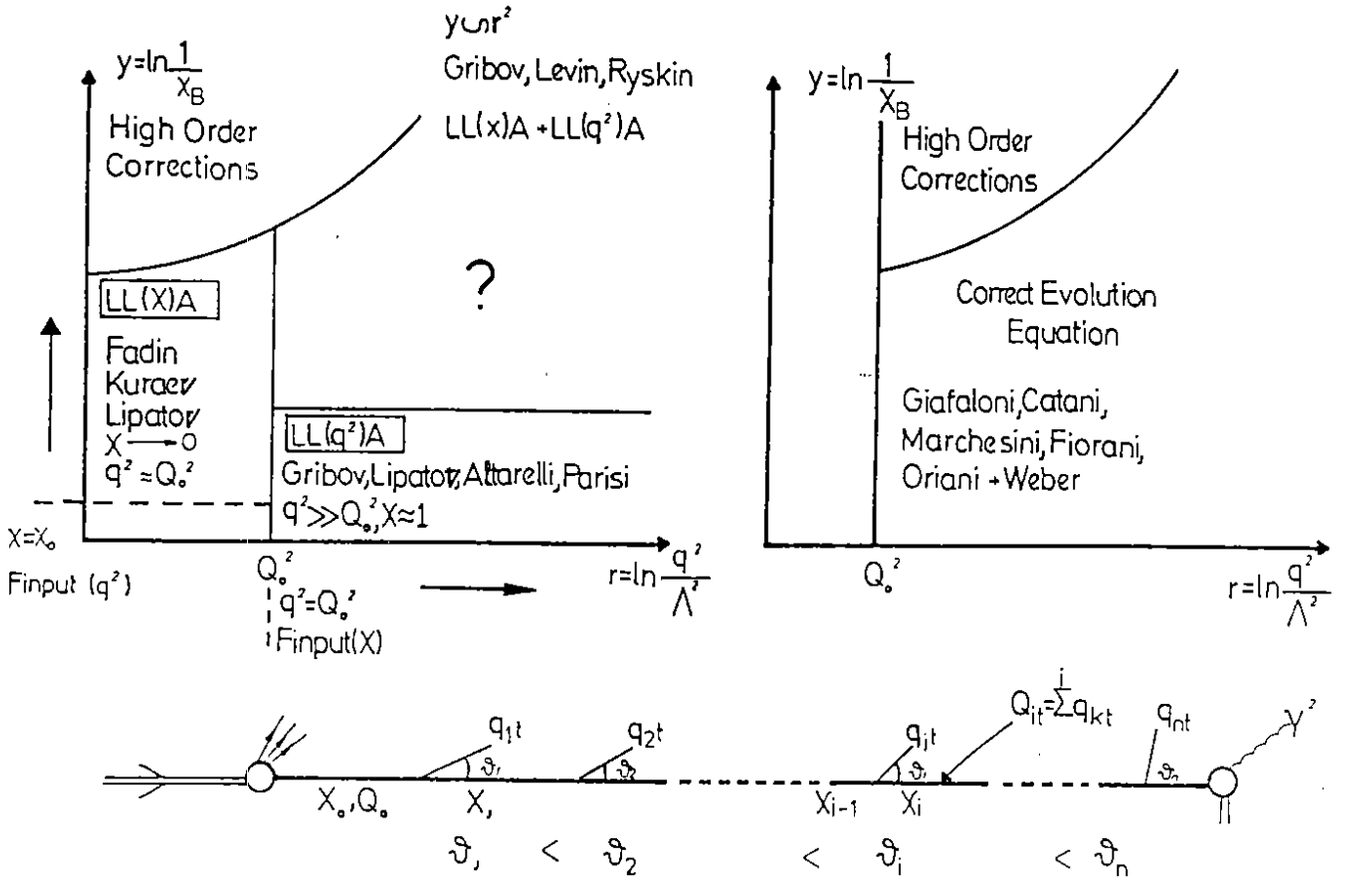
y=ln 1/x_B
High Order Corrections
y∼r²
Gribov, Levin, Ryskin
LL(x)A + LL(q²)A
?
LL(X)A
Fadin
Kuraev
Lipatov
X → 0
q² ≈ Q₀²
LL(q²)A
Gribov, Lipatov, Altarelli, Parisi
q² ≫ Q₀², X≈1
X=X₀
Finput (q²)
Q₀²
q²=Q₀²
Finput(X)
r=ln q²/Λ²
y=ln 1/x_B
High Order Corrections
Correct Evolution Equation
Giafaloni, Catani, Marchesini, Fiorani, Oriani + Weber
Q₀²
r=ln q²/Λ²
q₁t
q₂t
q_it
Q_it=Σ q_kt
q_nt
γ*
X₀, Q₀
X₁
X_{i-1}
X_i
ϑ₁ < ϑ₂ < ϑ_i < ϑ_n

Fig.2.

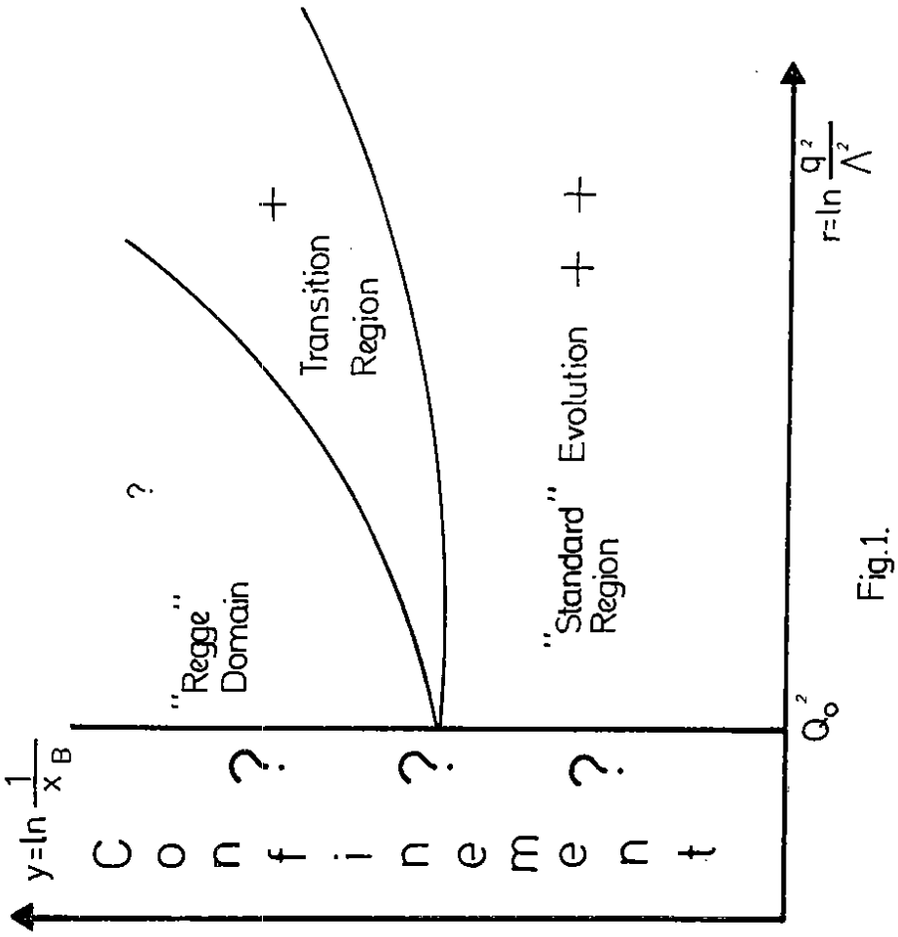
y=ln 1/x_B
Confinement
"Regge" Domain
?
Transition Region
+
"Standard" Evolution
+ +
Q₀²
r=ln q²/Λ²

Fig.1.

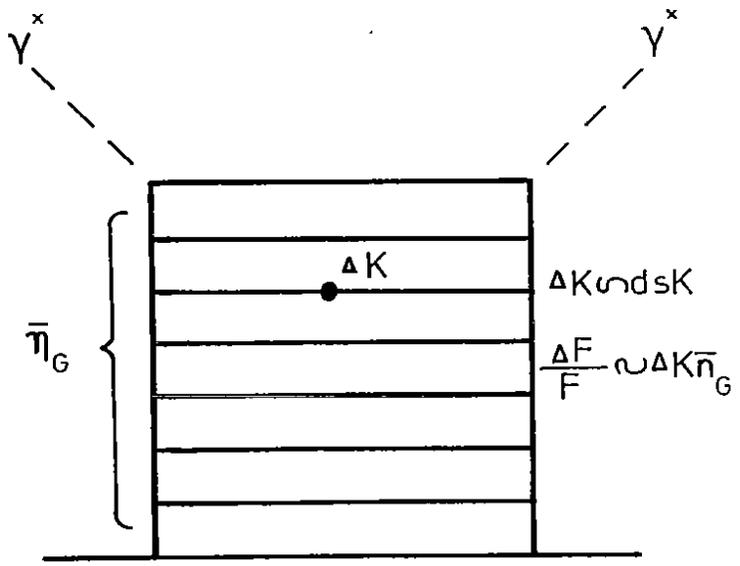
γ*
γ*
ΔK
ΔK∪dsK
$\bar{\eta}_G$
$\frac{\Delta F}{F} \sim \Delta K \bar{n}_G$

Fig. 3

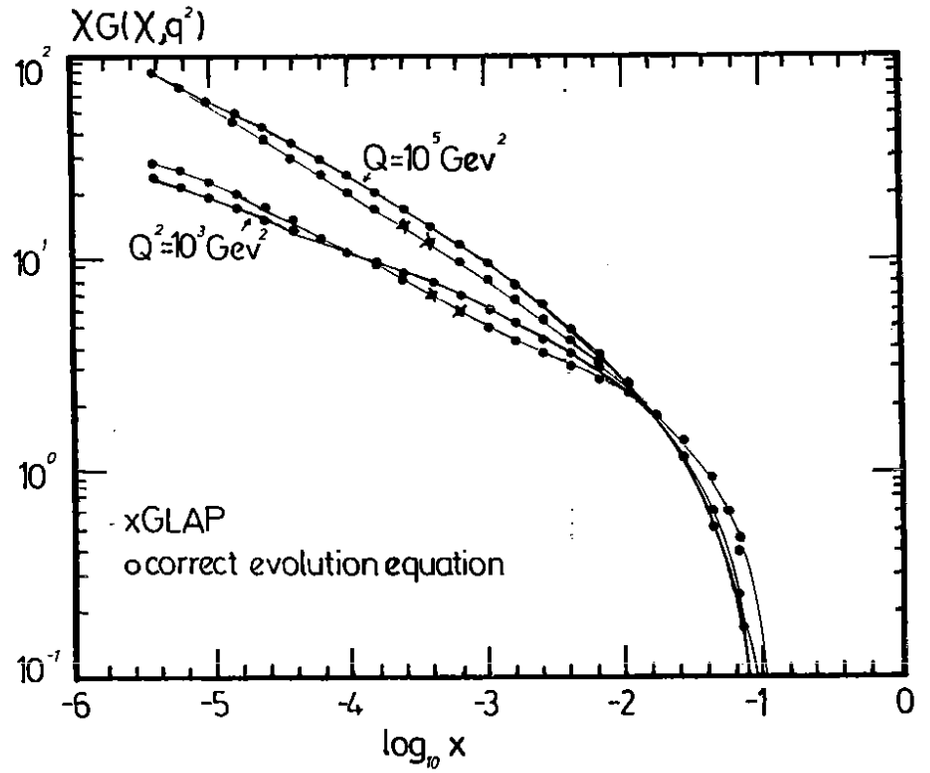
XG(X,q²)
10²
10¹
10⁰
10⁻¹
Q=10⁵Gev²
Q²=10³Gev²
xGLAP
o correct evolution equation
-6
-5
-4
-3
-2
-1
0
log₁₀ x

Fig.4.

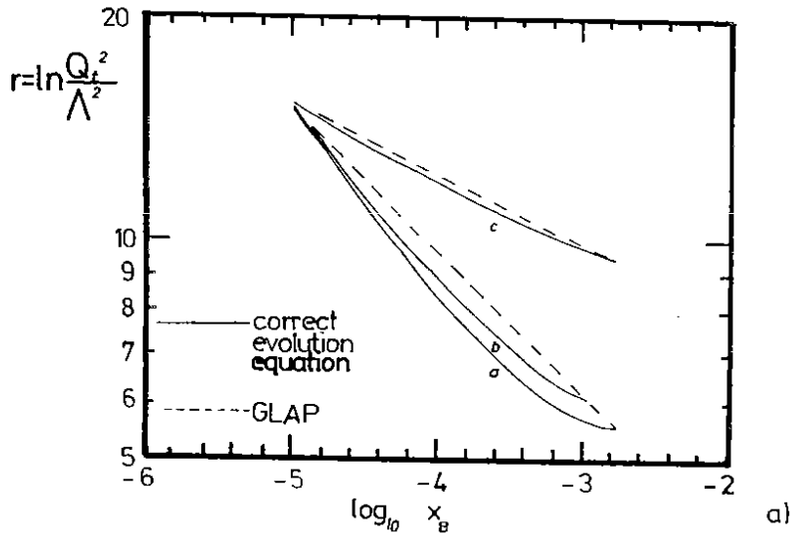

a)

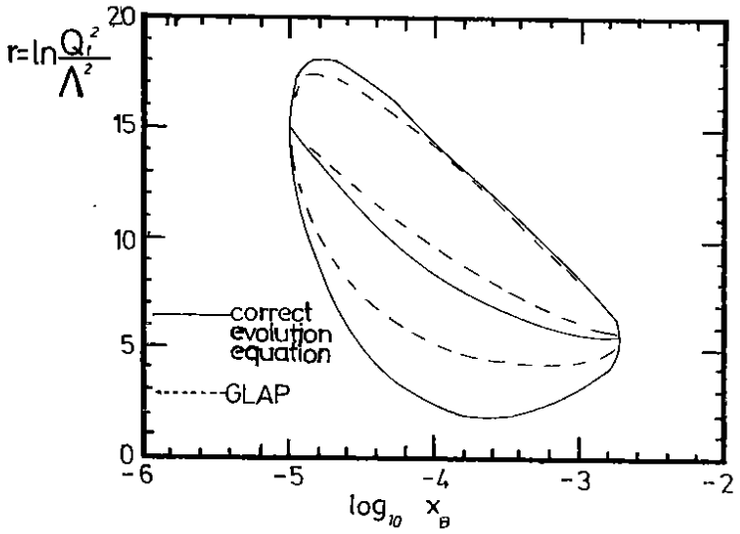

b)

Fig.5.

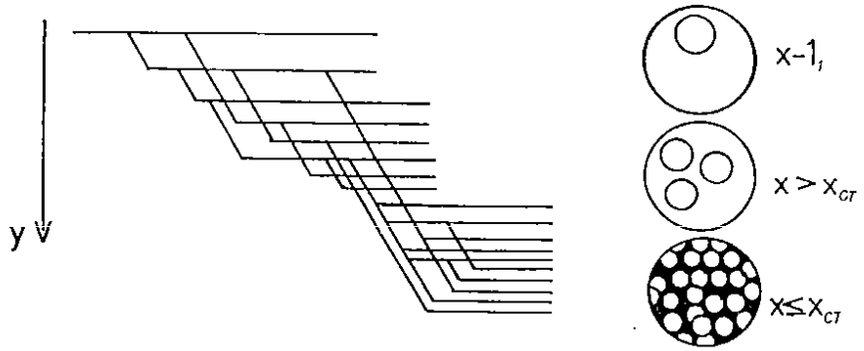

Fig.6.

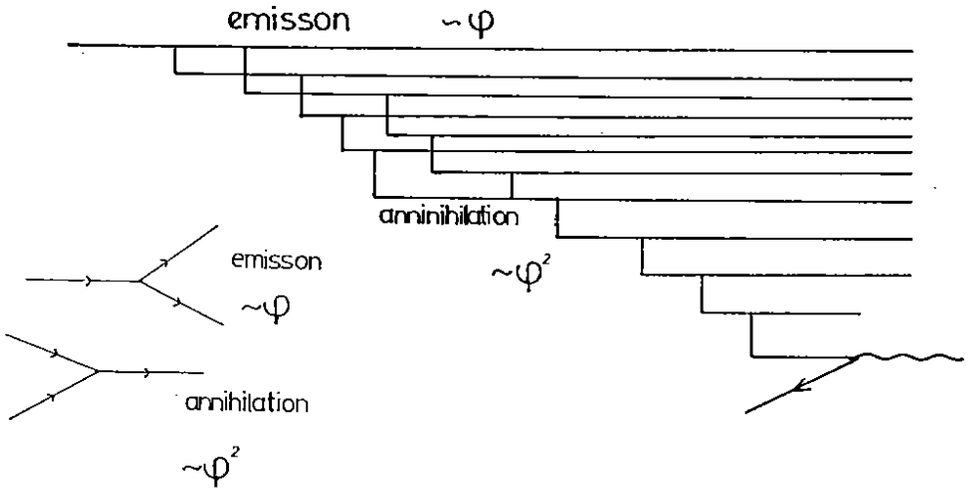

Fig.7.

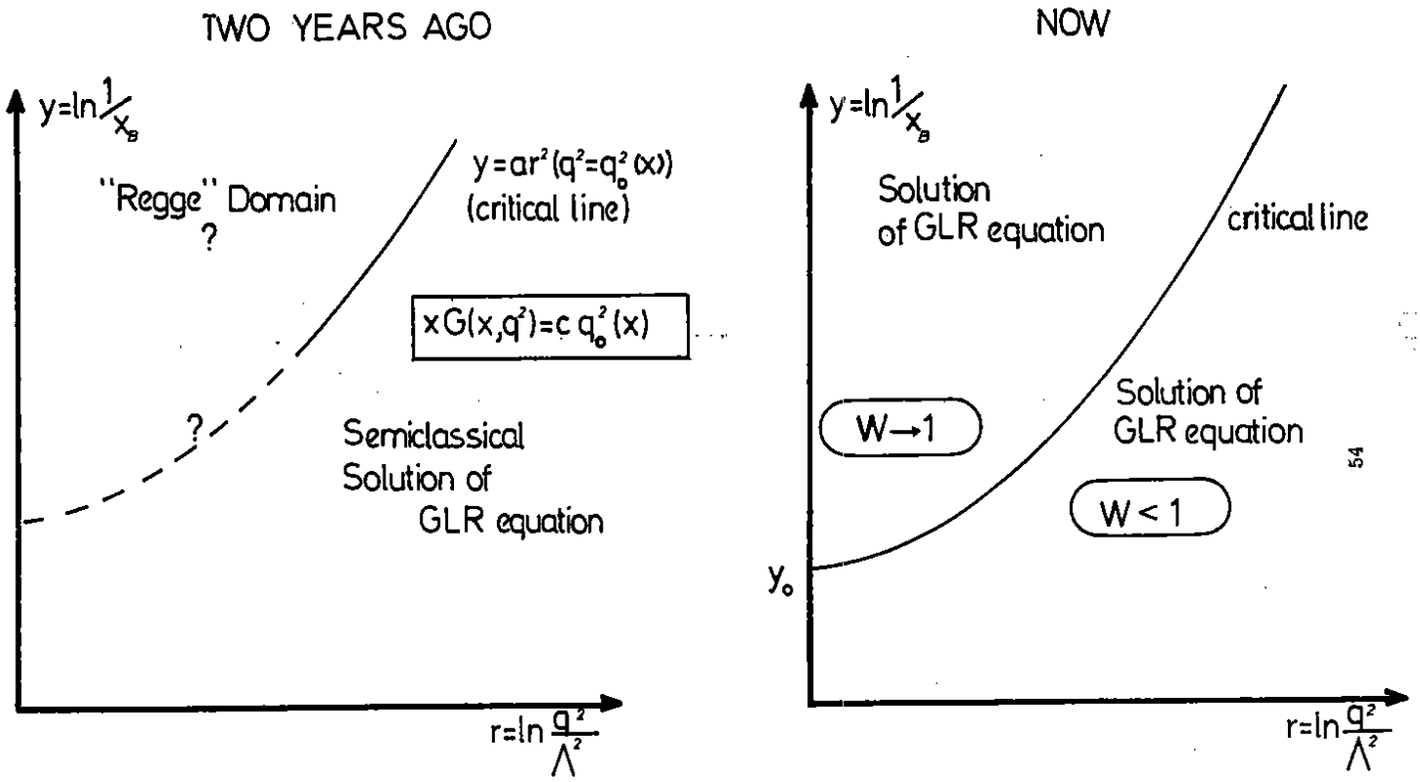

Fig.10.

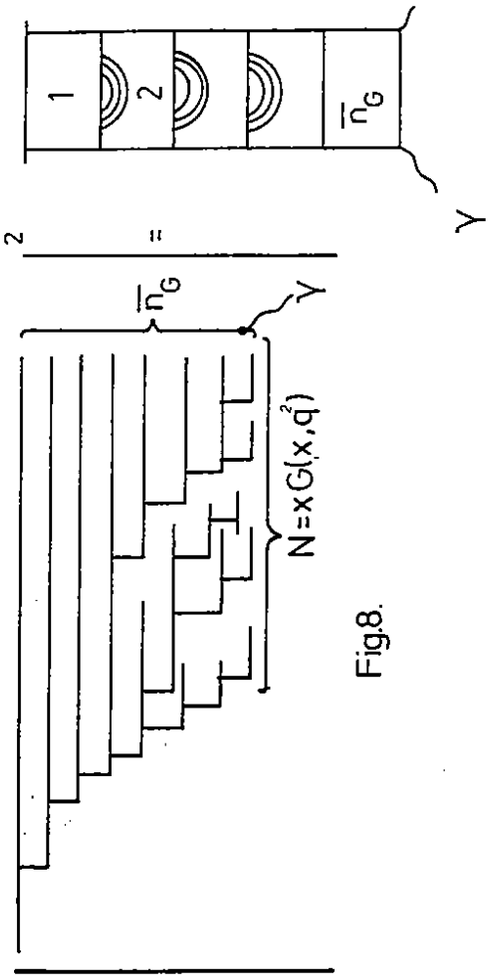

Fig.8.

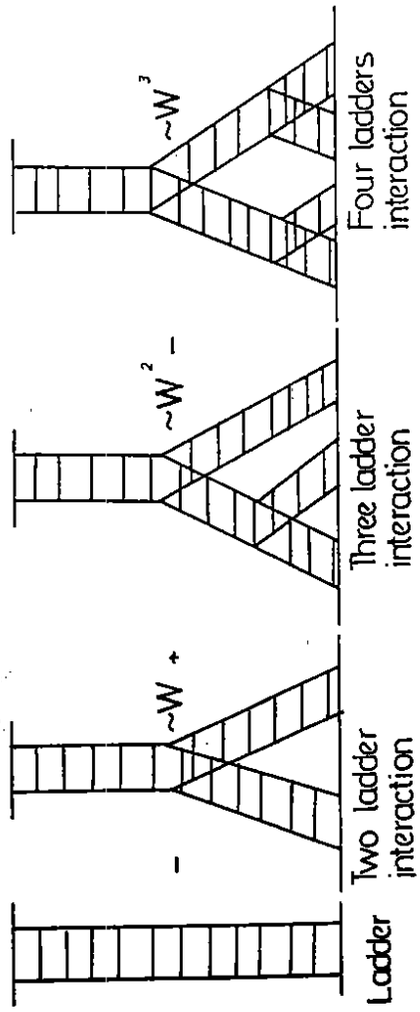

Fig.9.

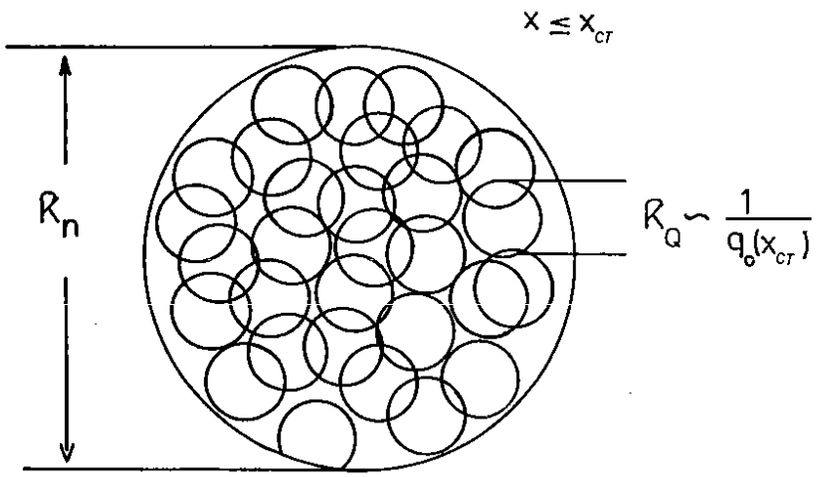

Fig.11.

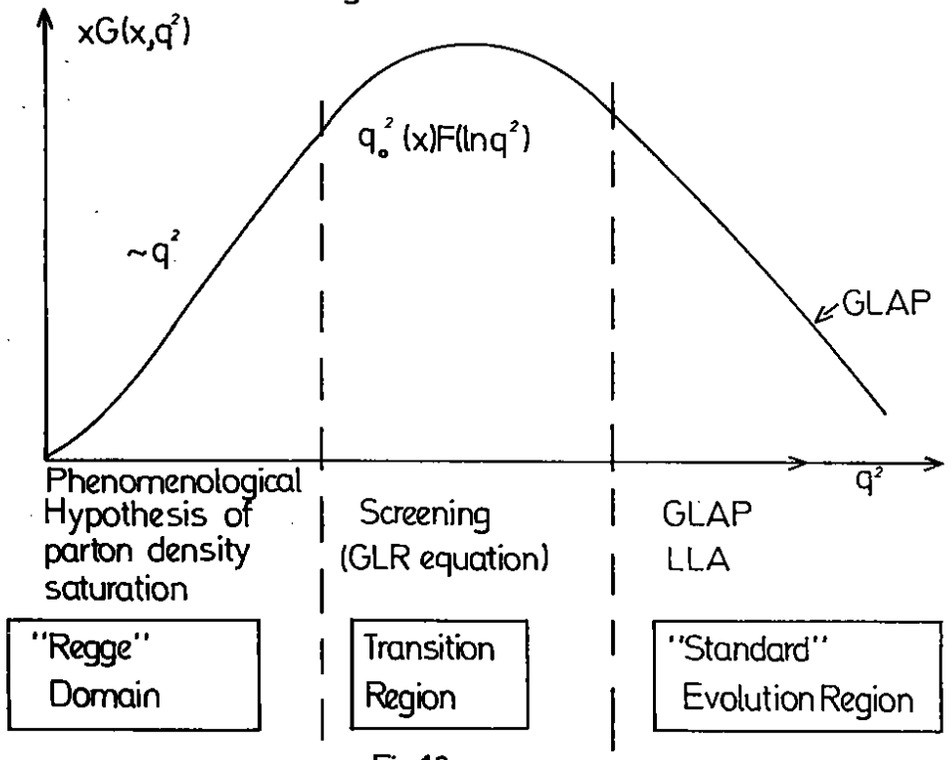

Fig.12.

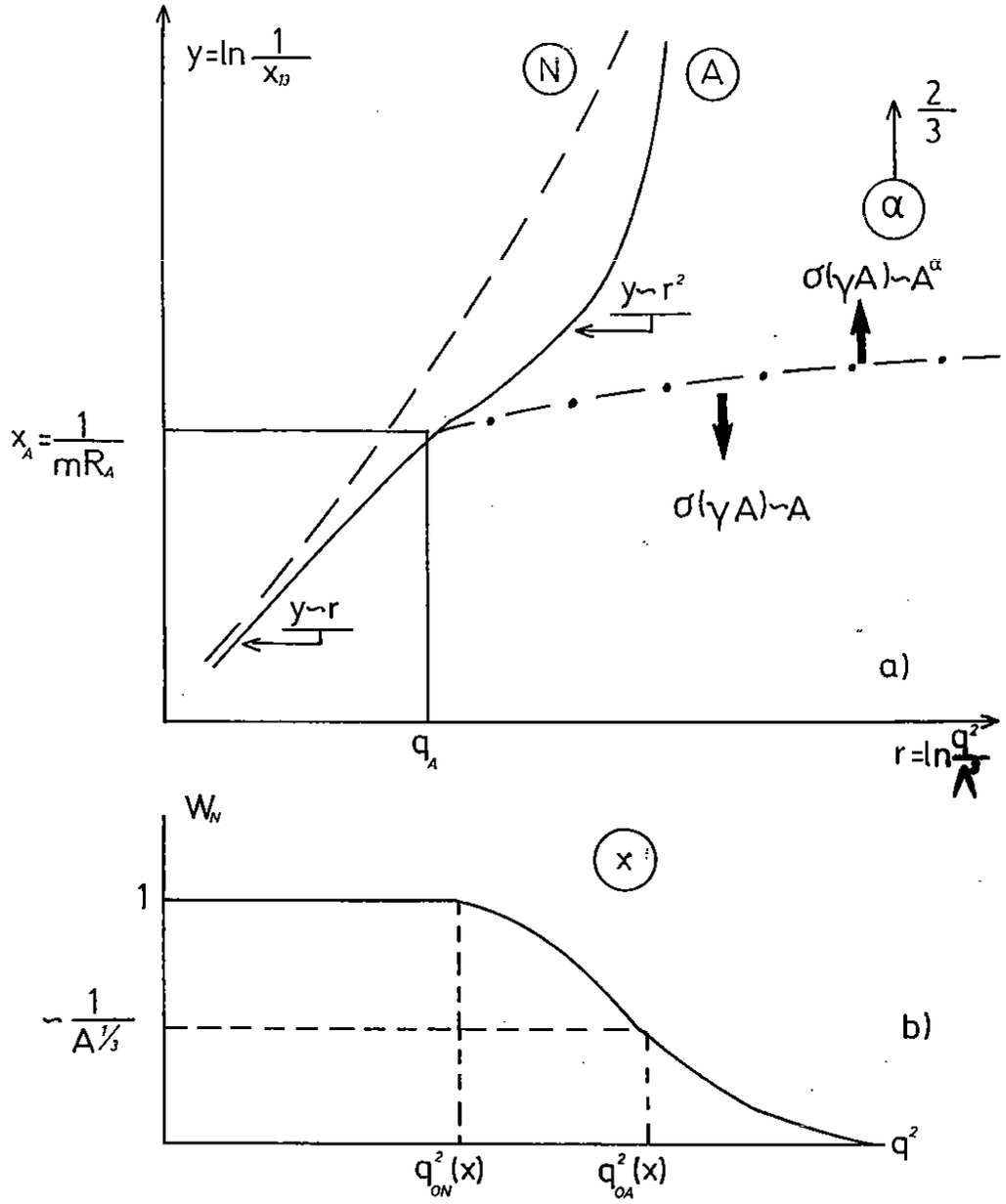

Fig.13.

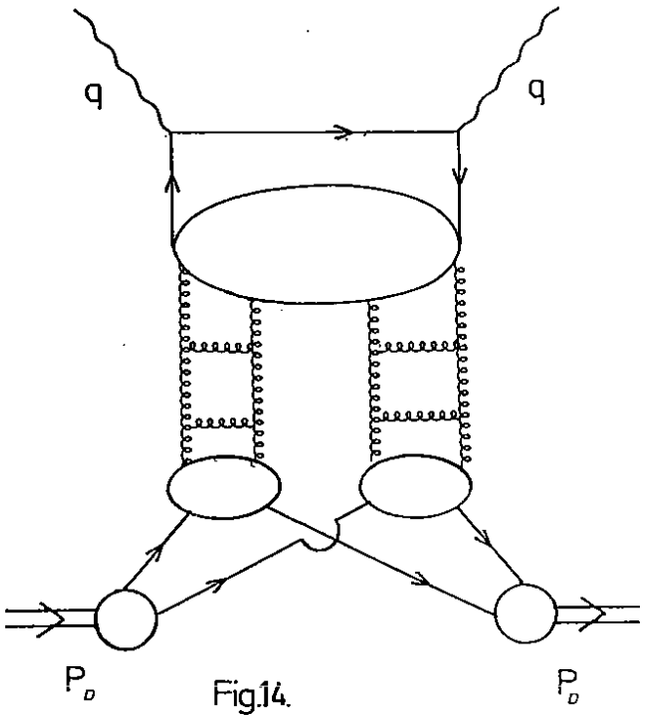

Fig.14.

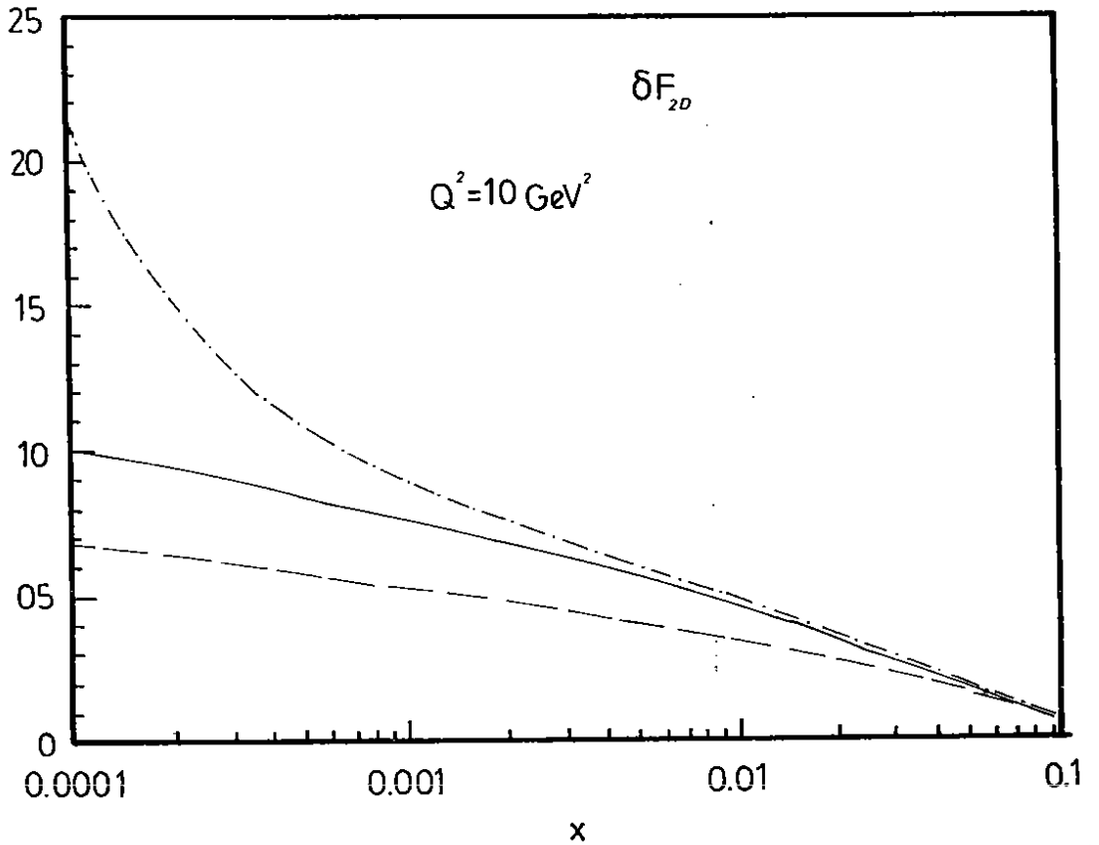

Fig.15.

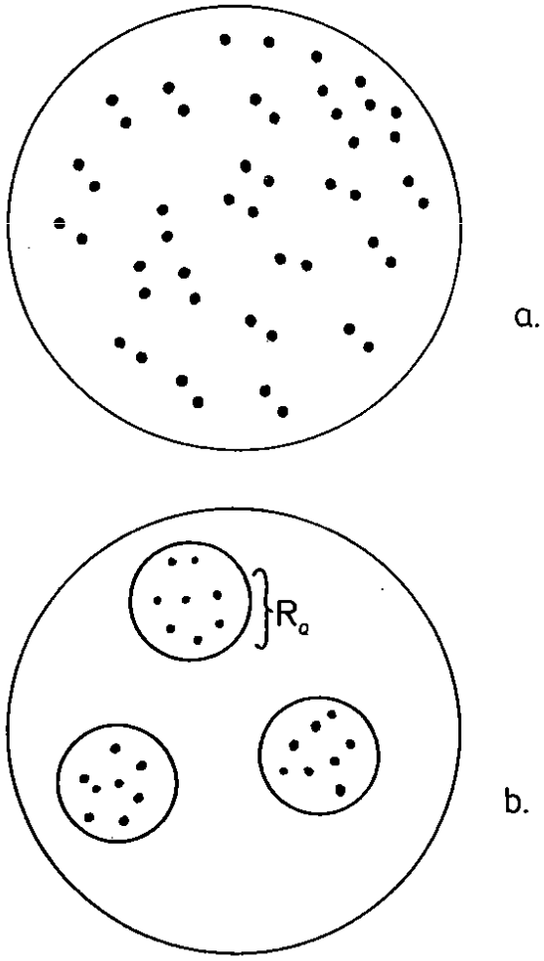
a.
R_Q
b.

Fig.16.

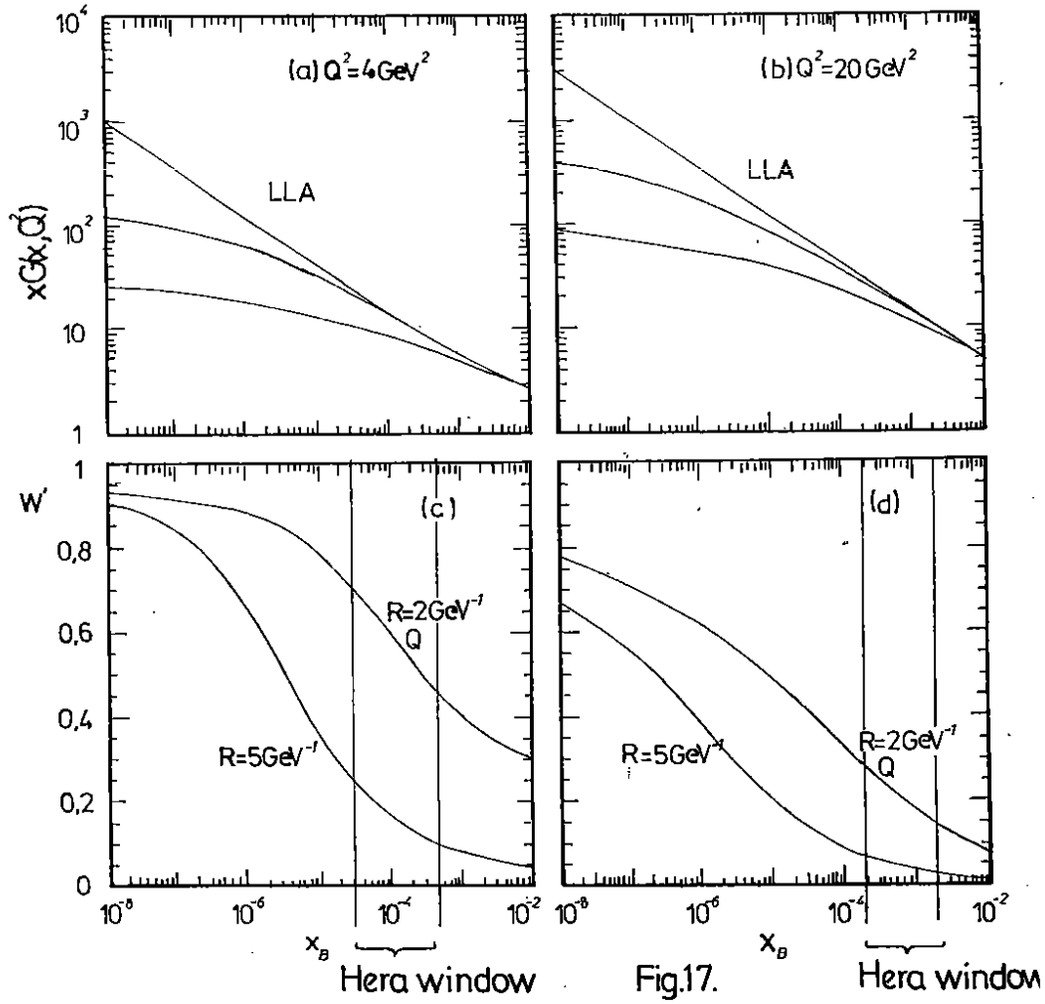
(a) $Q^2=4GeV^2$
(b) $Q^2=20GeV^2$
LLA
LLA
$xG(x,Q^2)$
10^4
10^3
10^2
10
1
W'
1
0,8
0,6
0,4
0,2
0
(c)
(d)
$R=2GeV^{-1}$
Q
$R=5GeV^{-1}$
$R=5GeV^{-1}$
$R=2GeV^{-1}$
Q
10^{-8}
10^{-6}
10^{-4}
10^{-2}
x_B
Hera window
10^{-8}
10^{-6}
10^{-4}
10^{-2}
x_B
Hera window

Fig.17.

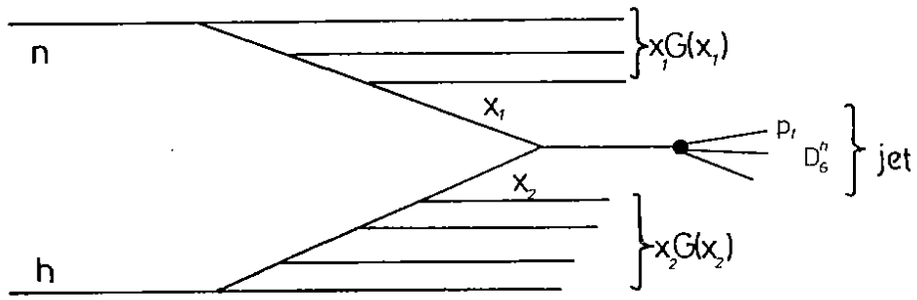
n
h
$x_1G(x_1)$
$x_2G(x_2)$
x_1
x_2
p_t
D_G^h
jet

Fig.18.

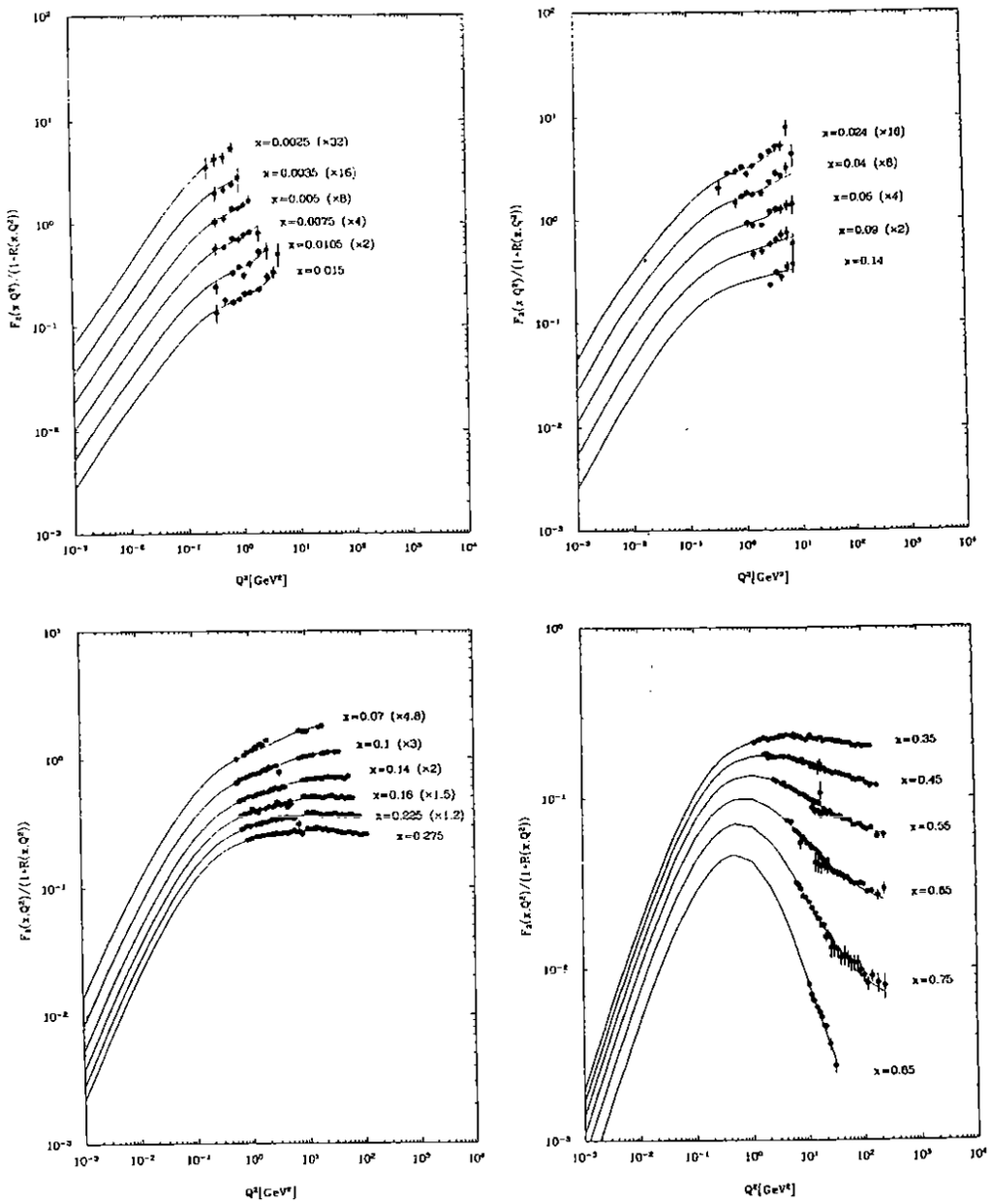
x=0.0025 (×32)
x=0.0035 (×16)
x=0.005 (×8)
x=0.0075 (×4)
x=0.0105 (×2)
x=0.015
x=0.024 (×16)
x=0.04 (×8)
x=0.06 (×4)
x=0.09 (×2)
x=0.14
x=0.07 (×4.8)
x=0.1 (×3)
x=0.14 (×2)
x=0.16 (×1.5)
x=0.225 (×1.2)
x=0.275
x=0.35
x=0.45
x=0.55
x=0.65
x=0.75
x=0.85
Q^2[GeV^2]

Fig. 19

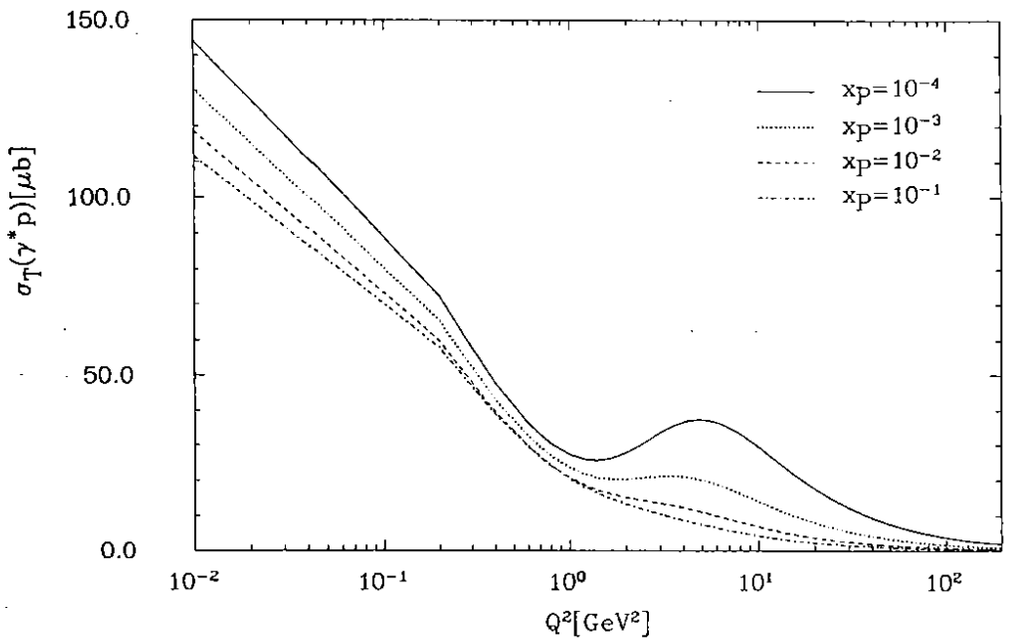
150.0
100.0
50.0
0.0
$\sigma_T(\gamma^* p)[\mu b]$
10^{-2}
10^{-1}
10^{0}
10^{1}
10^{2}
$Q^2[GeV^2]$
$x_P=10^{-4}$
$x_P=10^{-3}$
$x_P=10^{-2}$
$x_P=10^{-1}$

Fig. 20

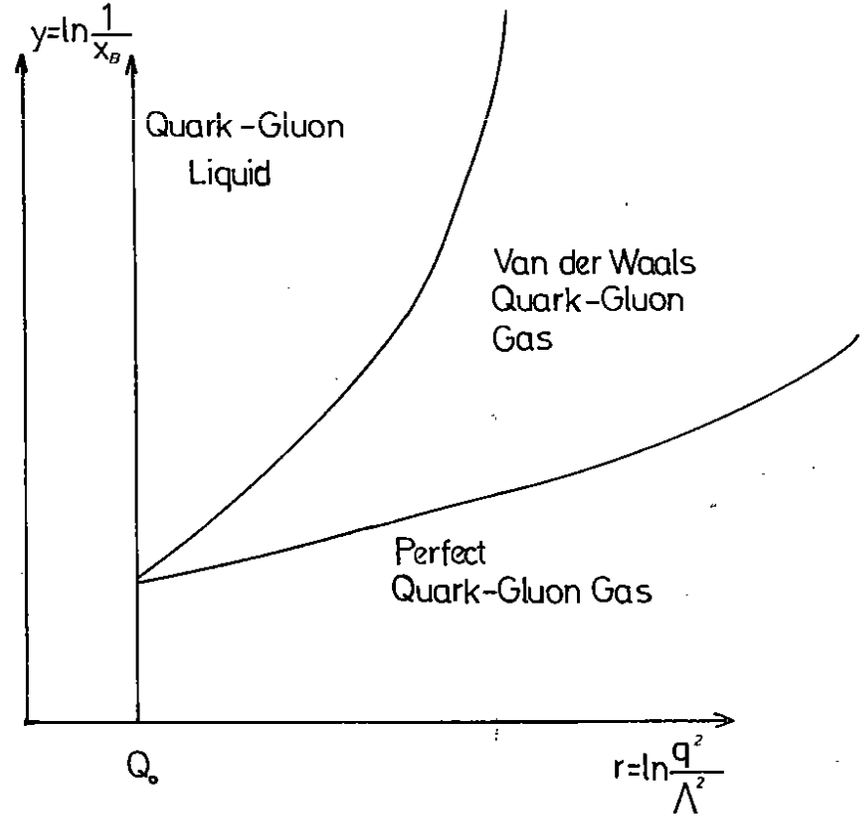
$y=\ln\frac{1}{x_B}$
Quark-Gluon
Liquid
Van der Waals
Quark-Gluon
Gas
Perfect
Quark-Gluon Gas
Q_0
$r=\ln\frac{Q^2}{\Lambda^2}$

Fig.21.

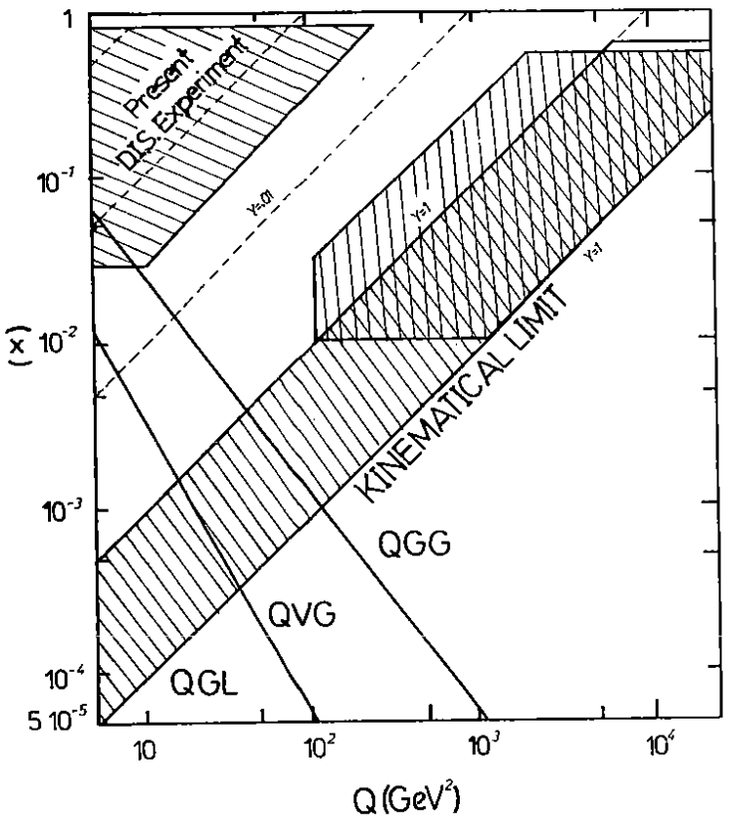

Fig. 22.

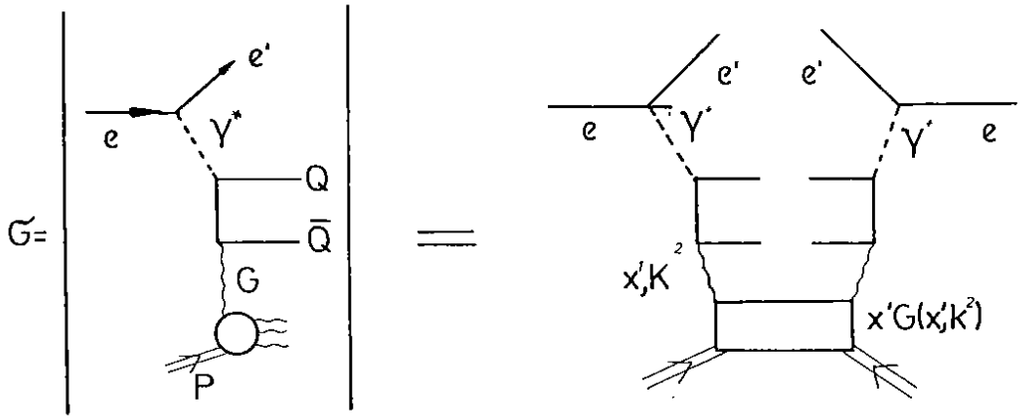

Fig. 23.

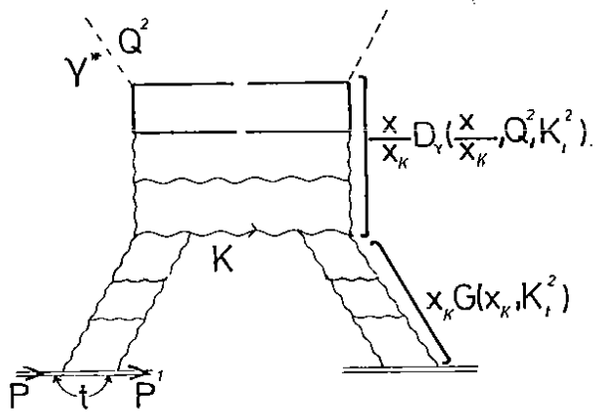

Fig. 24.

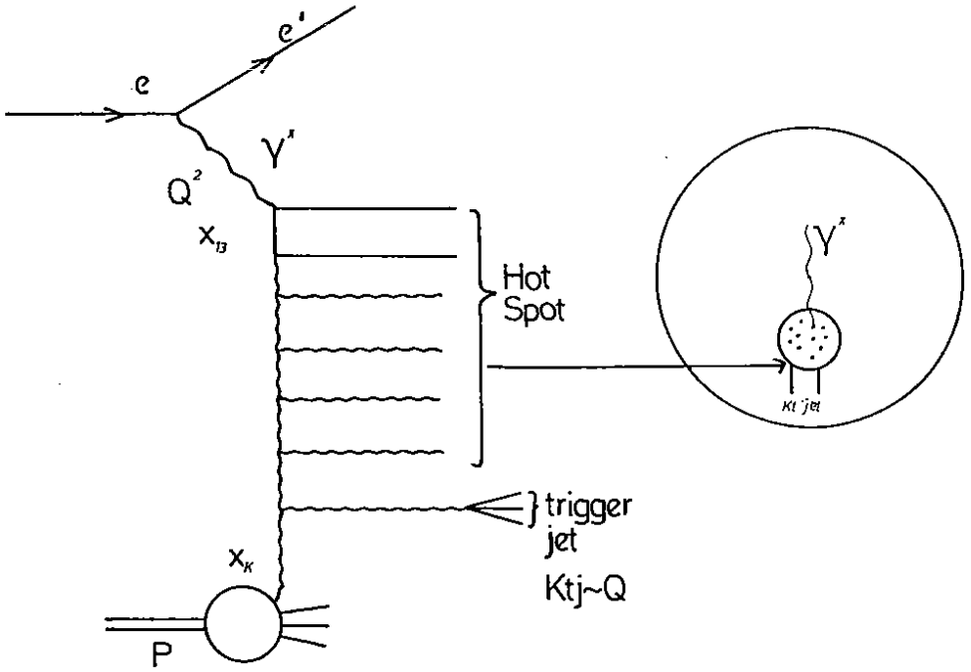
e
e'
γ*
Q²
x_B
Hot
Spot
γ*
Kt jet
} trigger
jet
Ktj~Q
x_K
P

Fig.25.

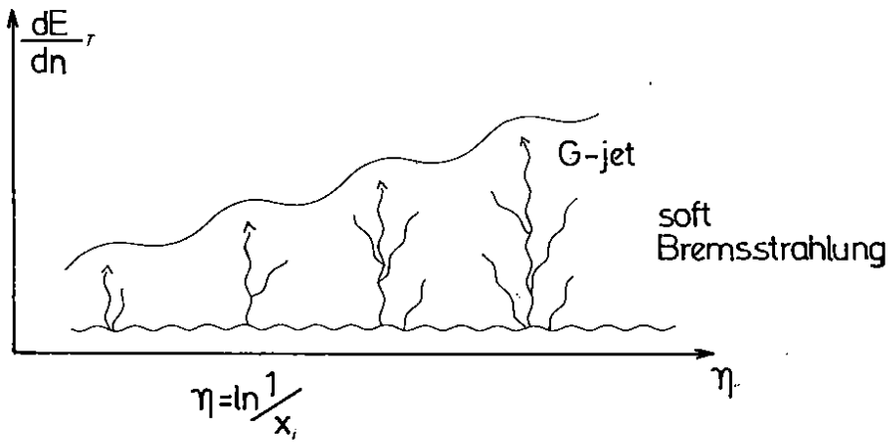
dE_T/dn
G-jet
soft
Bremsstrahlung
η=ln 1/x_i
η

Fig.26.

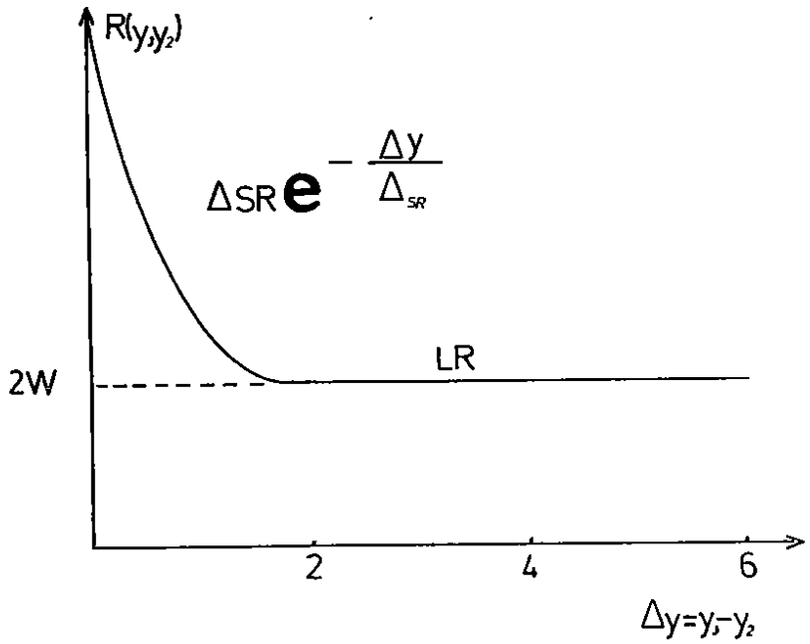
R(y,y₂)
ΔSR e^(−Δy/Δ_SR)
2W
LR
2
4
6
Δy=y₁−y₂

Fig.27.

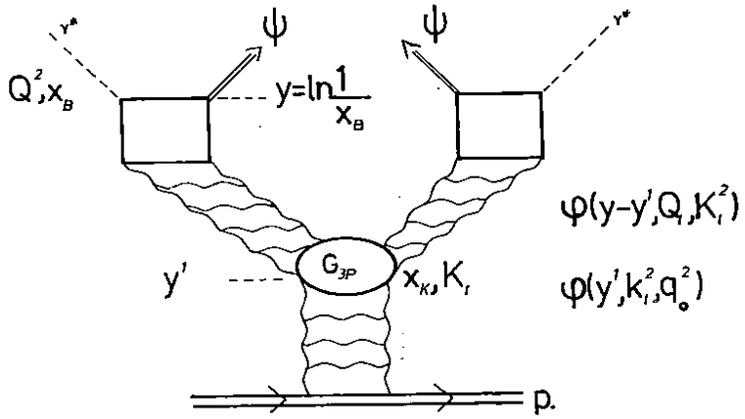
γ*
ψ
ψ
γ*
Q²,x_B
y=ln 1/x_B
φ(y−y',Q,K_t²)
y'
G_3P
x_K,K_t
φ(y',k_t²,q_0²)
p.

Fig.28.

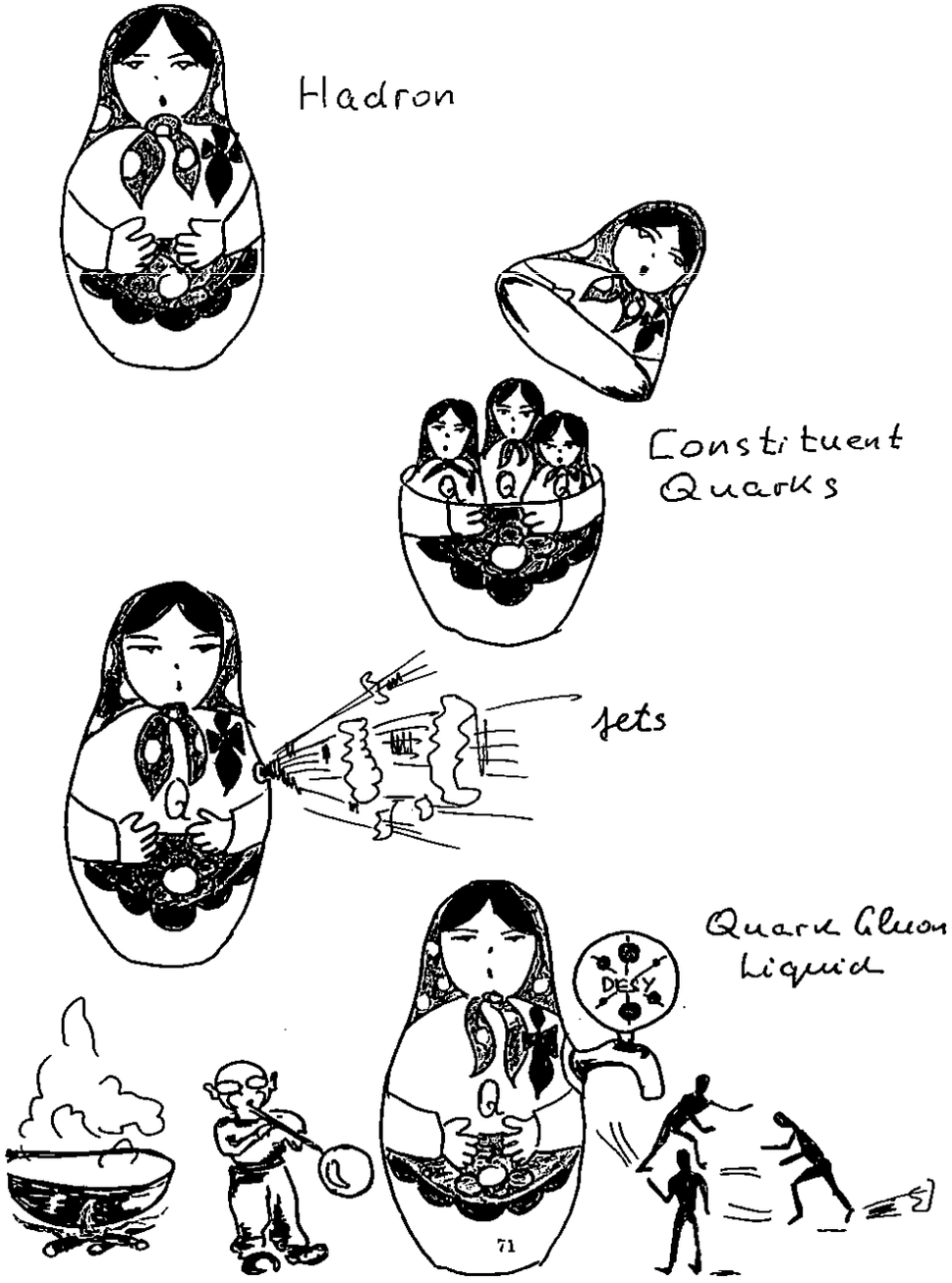
Hadron
Constituent Quarks
Q Q Q
Jets
Q
Quark Gluon Liquid
DESY
Q
71

Fig. 29